Contribution of single mutations to selected SARS-CoV-2 emerging variants Spike antigenicity

Shang Yu Gong[1,2]*, Debashree Chatterjee[1]*, Jonathan Richard[1,3], Jérémie Prévost[1,3], Alexandra Tauzin[1,3], Romain Gasser[1,3], Yuxia Bo[4] Dani Vézina[1,3], Guillaume Goyette[1], Gabrielle Gendron-Lepage[1], Halima Medjahed[1], Michel Roger[1,3,5], Marceline Côté[4], and Andrés Finzi[1,2,3]

[1]Centre de Recherche du CHUM, QC H2X 0A9, Canada
[2]Department of Microbiology and Immunology, McGill University, Montreal, QC H3A 0G4, Canada.
[3]Département de Microbiologie, Infectiologie et Immunologie, Université de Montréal, Montréal, QC H2X 0A9, Canada
[4] Department of Biochemistry, Microbiology and Immunology, and Center for Infection, Immunity, and Inflammation, University of Ottawa, Ottawa, ON K1H 8M5, Canada.
[5] Laboratoire de Santé Publique du Québec, Institut Nationale de Santé Publique du Québec, Sainte-Anne-de-Bellevue, QC H9X 3R5, Canada.

*Contributed equally

Corresponding author: Andrés Finzi andres.finzi@umontreal.ca

Key Words: Coronavirus, COVID-19, SARS-CoV-2, Spike glycoproteins, RBD, ACE2, temperature, variants of concern, vaccines

Word count for the abstract: 148

Character count for the text: 4079

ABSTRACT

Towards the end of 2020, multiple variants of concern (VOCs) and variants of interest (VOIs) have arisen from the original SARS-CoV-2 Wuhan-Hu-1 strain. Mutations in the Spike protein are highly scrutinized for their impact on transmissibility, pathogenesis and vaccine efficacy. Here, we contribute to the growing body of literature on emerging variants by evaluating the impact of single mutations on the overall antigenicity of selected variants and their binding to the ACE2 receptor. We observe a differential contribution of single mutants to the global variants phenotype related to ACE2 interaction and antigenicity. Using biolayer interferometry, we observe that enhanced ACE2 interaction is mostly modulated by a decrease in off-rate. Finally, we made the interesting observation that the Spikes from tested emerging variants bind better to ACE2 at 37°C compared to the D614G variant. Whether improved ACE2 binding at higher temperature facilitates emerging variants transmission remain to be demonstrated.

INTRODUCTION

Severe Acute Respiratory Syndrome Coronavirus 2 (SARS-CoV-2), the causative agent of COVID-19, remains an major public health concern, infecting over 185 million individuals and causing over 4 million deaths worldwide (Dong et al., 2020). The replication cycle of SARS-CoV-2 starts with viral attachment to the target cell and fusion between viral and cellular membranes. The viral entry process is mediated by the mature Spike (S) glycoprotein trimer which is composed of exterior S1 and transmembrane S2 subunits. The S1 subunit mediates attachment using its receptor-binding domain (RBD) to interact with the host protein angiotensin converting enzyme 2 (ACE2) (Hoffmann et al., 2020; Shang et al., 2020; Walls et al., 2019), while the S2 subunit governs the fusion between the viral and cellular membranes (Walls et al., 2020; Wrapp et al., 2020).The Spike is a major target of the cellular and humoral responses elicited by natural infection. Accordingly, the antigen used in currently approved vaccines is the stabilized form of the SARS-CoV-2 S glycoprotein. These vaccines use adenoviral vectors (Sadoff et al., 2021a; Voysey et al., 2021) or mRNA vaccine platforms to express S glycoprotein (Baden et al., 2020; Polack et al., 2020). The S glycoprotein was selected due to its high immunogenicity and safety profiles after extensive research (Jackson et al., 2020; Krammer, 2020; Mulligan et al., 2020; Sadoff et al., 2021b).

Although the approval of several vaccine platforms has given us hope to end the pandemic, the asymmetric distribution of doses between rich and poor countries and the rapid emergence of SARS-CoV-2 variants is preoccupying. The Spike is under high selective pressure to evade host immune response, improve ACE2 affinity, escape antibody recognition and achieve high transmissibility (Prévost and Finzi, 2021). The first identified D614G mutation in the Spike glycoprotein became dominant among the rapidly spreading emerging variants (Korber et al., 2020; Plante et al., 2021). In late 2020, several other variants emerged throughout the world, including

the variants of concern (VOCs) B.1.1.7 (Alpha), B.1.351 (Beta), P.1 (Gamma) and B.1.617.2 (Delta), as well as the variants of interest (VOIs) B.1.429 (Epsilon), B.1.526 (Iota), B.1.617.1 (Kappa) and B.1.617 (CDC; Deng et al., 2021; ECDC, 2020, 2021; Ferreira et al., 2021; Mwenda M, 2021; West et al., 2021). Critical mutations providing a fitness increase became rapidly selected in most emerging variants. For example, the N501Y substitution that was first observed in the B.1.1.7 lineage and provides enhanced ACE2 binding (Prévost et al., 2021; Starr et al., 2020; Zhu et al., 2021), is now present in B.1.351, P.1, and P.3 lineages. Similarly, the E484K and K417N/T mutations in the RBD that were first described in the B.1.351 and P.1 lineages likely due to immune evasion from vaccine or natural infection-elicited antibodies (Amanat et al., 2021; Wang et al., 2021), are now present in several other lineages (Rambaut et al., 2020). Hence, it is important to closely monitor not only the emerging variants but also single mutations to better understand their contribution to replicative fitness and/or ability to evade natural or vaccine-induced immunity.

Here, by performing detailed binding and neutralization experiments with plasma from naturally infected and vaccinated individuals, we provide a comprehensive analysis of the antigenicity of the Spike from selected VOCs (B.1.1.7, B.1.351, P.1 and B.1.617.2) and VOIs (B.1.429, B.1.526, B.1.617, B.1.617.1).

MATERIALS AND METHODS

Ethics Statement

All work was conducted in accordance with the Declaration of Helsinki in terms of informed consent and approval by an appropriate institutional board. Blood samples were obtained from donors who consented to participate in this research project at CHUM (19.381). Plasmas were isolated by centrifugation.

Plasmas and antibodies

Plasmas of SARS-CoV-2 naïve-vaccinated and previously infected pre- and post-first dose vaccination donors were collected, heat-inactivated for 1 hour at 56°C and stored at -80°C until use in subsequent experiments. Plasma from uninfected donors collected before the pandemic were used as negative controls in our flow cytometry and neutralization assays (not shown). The S2-specific monoclonal antibody CV3-25 was used as a positive control and to normalized Spike expression in our flow cytometry assays and was previously described (Jennewein et al., 2021; Mothes et al., 2021; Tauzin et al., 2021; Ullah et al., 2021). ACE2 binding was measured using the recombinant ACE2-Fc protein, which is composed of two ACE2 ectodomains linked to the Fc portion of the human IgG (Anand et al., 2020).Alexa Fluor-647-conjugated goat anti-human Abs (Invitrogen) were used as secondary antibodies to detect ACE2-Fc and plasma binding in flow cytometry experiments.

Cell lines

293T human embryonic kidney cells (obtained from ATCC) were maintained at 37°C under 5% CO_2 in Dulbecco's modified Eagle's medium (DMEM) (Wisent) containing 5% fetal bovine serum

(VWR) and 100 µg/ml of penicillin-streptomycin (Wisent). The 293T-ACE2 cell line was previously described (Prévost et al., 2020) and was maintained in medium supplemented with 2 µg/mL of puromycin (Millipore Sigma).

Plasmids

The plasmid encoding B.1.1.7, B.1.351, P.1, and B.1.526 Spikes were codon-optimized and synthesized by Genscript. Plasmids encoding B.1.617, B.1.617.1, B.1.617.2 Spikes were generated by overlapping PCR using a codon-optimized wild-type SARS-CoV-2 Spike gene (GeneArt, ThermoFisher) that was synthesized (Biobasic) and cloned in pCAGGS as a template. Plasmids encoding B.1.429, D614G and other SARS-CoV-2 Spike single mutations were generated using the QuickChange II XL site-directed mutagenesis protocol (Stratagene) and the pCG1-SARS-CoV-2-S plasmid kindly provided by Stefan Pöhlmann. The presence of the desired mutations was determined by automated DNA sequencing.

Protein expression and purification

FreeStyle 293F cells (Invitrogen) were grown in FreeStyle 293F medium (Invitrogen) to a density of 1 x 10^6 cells/mL at 37°C with 8 % CO_2 with regular agitation (150 rpm). Cells were transfected with a plasmid coding for SARS-CoV-2 S RBD using ExpiFectamine 293 transfection reagent, as directed by the manufacturer (Invitrogen). One week later, cells were pelleted and discarded. Supernatants were filtered using a 0.22 µm filter (Thermo Fisher Scientific). The recombinant RBD proteins were purified by nickel affinity columns, as directed by the manufacturer (Invitrogen). The RBD preparations were dialyzed against phosphate-buffered saline (PBS) and

stored in aliquots at -80°C until further use. To assess purity, recombinant proteins were loaded on SDS-PAGE gels and stained with Coomassie Blue.

Virus neutralization assay

293T cells were transfected with the lentiviral vector pNL4.3 R-E- Luc (NIH AIDS Reagent Program) and a plasmid encoding for the indicated Spike glycoprotein (D614G, B.1.1.7, P.1, B.1.351, B.1.429, B.1.526, B.1.617, B.1.617.1, B.1.617.2) at a ratio of 10:1. Two days post-transfection, cell supernatants were harvested and stored at -80°C until use. 293T-ACE2 target cells were seeded at a density of 1×10^4 cells/well in 96-well luminometer-compatible tissue culture plates (Perkin Elmer) 24h before infection. Pseudoviral particles were incubated with the indicated plasma dilutions (1/50; 1/250; 1/1250; 1/6250; 1/31250) for 1h at 37°C and were then added to the target cells followed by incubation for 48h at 37°C. Then, cells were lysed by the addition of 30 µL of passive lysis buffer (Promega) followed by one freeze-thaw cycle. An LB942 TriStar luminometer (Berthold Technologies) was used to measure the luciferase activity of each well after the addition of 100 µL of luciferin buffer (15mM $MgSO_4$, 15mM KPO_4 [pH 7.8], 1mM ATP, and 1mM dithiothreitol) and 50 µL of 1mM d-luciferin potassium salt (Prolume). The neutralization half-maximal inhibitory dilution (ID_{50}) represents the plasma dilution to inhibit 50% of the infection of 293T-ACE2 cells by SARS-CoV-2 pseudoviruses.

Cell surface staining and flow cytometry analysis

293T were transfected with full length SARS-CoV-2 Spikes and a green fluorescent protein (GFP) expressor (pIRES2-eGFP; Clontech) using the calcium-phosphate method. Two days post-transfection, 293T-Spike cells were stained with the CV3-25 Ab, ACE2-Fc or plasma from SARS-

158 CoV-2-naïve or recovered donors. Briefly, 5 µg/mL CV3-25 or 20 µg/mL ACE2-Fc were
159 incubated with cells at 37ºC or 4 ºC for 45 min. Plasma from SARS-CoV-2 naïve or convalescent
160 donors were incubated with cells at 37ºC. The percentage of Spike-expressing cells (GFP+ cells)
161 was determined by gating the living cell population based on viability dye staining (Aqua Vivid,
162 Invitrogen). Samples were acquired on a LSRII cytometer (BD Biosciences), and data analysis
163 was performed using FlowJo v10.7.1 (Tree Star). The conformational-independent S2-targeting
164 mAb CV3-25 was used to normalize Spike expression. CV3-25 was shown to be effective against
165 all Spike variants (Mothes et al., 2021). The Median Fluorescence intensities (MFI) obtained with
166 ACE2-Fc or plasma Abs were normalized to the MFI obtained with CV3-25 and presented as ratio
167 of the CV3-25-normalized values obtained with the D614G Spike.
168
169 **Biolayer Interferometry**
170 Binding kinetics were performed on an Octet RED96e system (FortéBio) at 25°C with shaking at
171 1,000 RPM. Amine Reactive Second-Generation (AR2G) biosensors were hydrated in water, then
172 activated for 300 s with an S-NHS/EDC solution (Fortébio) prior to amine coupling. SARS-CoV-
173 2 RBD proteins were loaded into AR2G biosensor at 12.5 µg/mL in 10mM acetate solution pH5
174 (Fortébio) for 600 s and then quenched into 1M ethanolamine solution pH8.5 (Fortébio) for 300 s.
175 Baseline equilibration was collected for 120 s in 10X kinetics buffer. Association of sACE2 (in
176 10X kinetics buffer) to the different RBD proteins was carried out for 180 s at various
177 concentrations in a two-fold dilution series from 500nM to 31.25nM prior to dissociation for 300
178 s. The data were baseline subtracted prior to fitting performed using a 1:1 binding model and the
179 FortéBio data analysis software. Calculation of on-rates (K_a), off-rates (K_{dis}), and affinity constants
180 (K_D) was computed using a global fit applied to all data.

RESULTS

ACE2 recognition by SARS-CoV-2 single mutants and full Spike variants

Since the SARS-CoV-2 Spike is under strong selective pressure and is responsible for interacting with the ACE2 receptor, we measured the ability of the Spike from emerging variants to interact with ACE2 and the contribution of each single mutations toward this binding. Plasmids expressing the SARS-CoV-2 full Spike harboring single or combined mutations from emerging variants were transfected into HEK 293T cells. Spike expression was normalized with the conformationally independent, S2-specific CV3-25 monoclonal antibody (mAb) (Mothes et al., 2021; Ullah et al., 2021). ACE2 binding was measured using the recombinant ACE2-Fc protein, which is composed of two ACE2 ectodomains linked to the Fc portion of the human IgG (Anand et al., 2020). Alexa Fluor 647-conjugated secondary Ab was then used to detect ACE2-Fc binding to cell-surface Spike by flow cytometry. At the time of writing, B.1.617.1 and B.1.617.2 came into importance and only the full Spikes from these variants were synthesized, not the single mutations. When compared to the D614G Spike, all tested Spike variants, with the exception of B.1.617.1, presented significantly higher ACE2 binding (Fig 1A).

We then determine the contribution of individual Spike mutations on ACE2 binding to discern the ones contributing to the heightened receptor affinity of emerging variants. The B.1.1.7 Spike presented the highest ACE2-Fc interaction amongst all tested Spikes, which is a 5.43-fold increase in ACE2-Fc binding compared to D614G (Fig 1A-B and Table S2). The mutations that likely contribute to this phenotype are ΔH69-V70 in the N terminal domain (NTD) and N501Y in the RBD that enhanced binding by ~1.51 and ~2.52 folds, respectively (Fig 1B).

The Spike from B.1.351 also presented significantly higher ACE2-Fc binding compared to D614G. Similarly to B.1.1.7, the N501Y mutation likely plays an important role in this phenotype

(Fig. 1C). Interestingly, three mutations/deletion in this VOC decreased the interaction with ACE2-Fc, namely R246I and Δ242-244 in the NTD, as well as K417N in the RBD. The NTD substitution R246I decreased ACE2-Fc binding by ~1.52 folds , the Δ242-244 deletion by ~1.35 folds, whereas K417N had a greater impact with a decreased binding of ~7.7 folds relative to D614G (Fig 1C). Of note, the E484K mutation, also found in the RBD of other emerging variants (P.1 and B.1.526) did not significantly impact the ACE2-Fc interaction.

The Spike from P.1 presented a ~4.24-fold increase in binding compared to D614G (Fig 1D). Few NTD mutations, namely T20N, P26S, D138Y, and R190S, likely contributed to the increase in ACE2 binding, with ~2, ~1.6, ~1.3 and ~1.8- fold increase compared to D614G, respectively. Like the above-mentioned VOCs, N501Y also likely played a role in enhanced ACE2-Fc interaction. Interestingly, the RBD mutation K417T and the S2 mutation T1027I decreased the ACE2-Fc by ~1.3 and ~1.7 folds respectively. The H655Y mutation, near the S1/S2 cleavage site, also slightly increased ACE2 interaction by ~1.2 folds (Fig 1D).

The Spike from B.1.429 augmented ACE2-Fc interaction by ~2.8 folds (Fig 1E). This VOI has two NTD mutations, S13I and W152C, both of which did not significantly impact this interaction. On the other hand, its RBD mutation, L452R, increased ACE2-Fc binding by ~2.7 folds, suggesting its major contribution to the phenotype of this variant (Fig 1E).

Lastly, the Spike from B.1.526 showed a ~1.8-fold increase over D614G (Fig 1F). None of the mutation appears to explain the phenotype observed with the full variant.

While our results identified some key mutations enhancing ACE2 interaction (i.e., N501Y,L452R and mutation/deletion in the NTD), the overall increased ACE2 affinity from any given variant appears to result from more than the sum of the effect of individual mutations composing this variant.

228

229 **Impact of selected mutations on the affinity of Spike RBD for ACE2**

230 Next, we used biolayer interferometry (BLI) to measure the binding kinetics of selected
231 RBD mutants to soluble ACE2 (sACE2). Biosensors were coated with recombinant RBD and put
232 in contact with increasing concentration of sACE2 (Fig 2). In agreement with previous reports
233 (Prévost et al., 2021; Zhu et al., 2021), the N501Y mutation present in B.1.1.7, B.1.351, and P.1
234 significantly decreased the off-rate (K_{dis}) (from 6.88×10^{-3} to 1.49×10^{-3} 1/s), presenting a 3.88-fold
235 increase in K_D compared to its wild-type counterpart (Fig 2A-B, Table S1). Substitution at position
236 K417 (either N or T) present in B.1.351 or P.1 lineages accelerated the off-rate kinetics, resulting
237 in a 0.75- and 0.66-fold decrease in binding affinity (Fig 2C-D, Table S1). Although both K417N
238 and K417T presented a modest increase in the on-rate kinetic by ~1.56 and ~ 1.11 folds, the
239 accelerated off-rate kinetics dictated the overall decrease affinity of these mutants. No major
240 changes were observed for the E484K mutation (Fig 2F). Interestingly, the L452R mutant did not
241 have a major impact in ACE2 affinity when tested in the context of recombinant monomeric RBD
242 (Fig. 2G) but presented enhanced binding within the context of full-length membrane anchored
243 Spike (Fig. 1E), indicating that the overall phenotype of a mutant (in this case enhanced binding)
244 cannot always be recapitulated with the RBD alone. Altogether, our results show that at least for
245 the RBD mutants tested here, ACE2 affinity is mostly dictated by the dissociation kinetics.

246

247 **Effect of temperature on full variants Spike recognition of ACE2**

248 It was recently shown that the affinity of Spike for ACE2 increases at low temperatures
249 (Prévost et al., 2021). Interestingly, Prévost *et al*. also showed that the Spike from B.1.1.7 or
250 harboring the N501Y mutation present better ACE2 binding at higher temperatures compared to

the D614G strain (Prévost et al., 2021). To evaluate whether the Spikes from the emerging variants tested here also shared this phenotype, Spike-expressing cells were incubated at either 4ºC or 37ºC, and their ACE2-Fc binding was measured by flow cytometry. As presented in Fig. 3, the binding of ACE2-Fc to cell surface Spike was higher at cold temperature (4°C) compared to warm temperature (37°C) for all the variants. The impact of cold temperature on ACE2 binding was, however, more pronounced for the D614G Spike (3.62-fold increase) comparatively to Spikes from emerging variants (1.57 to 3.08-fold increase). While ACE2 displayed higher binding for the different emerging variants Spikes at 37ºC, similar level of binding could only be achieved for the D614G Spike when decreasing the temperature to 4°C. This suggests that Spikes from emerging variants are able to bypass the temperature restraint to achieve high ACE2 binding. Interestingly, variants harboring the N501Y mutation (B.1.1.7, B.1.351 and P.1) exhibited an increase in ACE2 binding compared to D614G Spike at both 4ºC and 37ºC, while this phenotype was only observed at 37ºC with Spike from the other variants. This indicate that the cold temperature and the N501Y mutation significantly impact Spike-ACE2 interaction.

Recognition of Spike variants by plasma from vaccinated individuals

To gain information related to the antigenic profile of each emerging variants Spike and their single mutants, we used plasma collected three weeks post BNT162b2 vaccination from SARS-CoV-2 naïve (Fig. 4) or previously-infected individuals (Fig. 5) (Tauzin et al., 2021). HEK 293T cells were transfected with Spike from emerging variants or their individual mutants and plasma binding was evaluated by flow cytometry, as previously reported (Anand et al., 2021; Beaudoin-Bussières et al., 2020; Gasser et al., 2021; Prévost et al., 2020; Tauzin et al., 2021). When compared to D614G, Spike from B.1.1.7, P.1 and the recently emerged B.1.617.1 and

B.1.617.2 variants were significantly less recognized by the plasma from SARS-CoV-2 naïve individuals (Fig 4A).

Mutations apparently contributing to the reduction of plasma recognition of the B.1.1.7 Spike are the ΔY144 deletion in the NTD, P681H and T716I near the S1/S2 cleavage site (Fig 4B). The N501Y substitution, also present in other emerging variants (B1.351 and P.1), is the only mutation that increased plasma recognition.

While we did not observe a significant decrease in plasma recognition of the B.1.351 Spike, most single mutants of this VOC (L18F, D80A, D215G, Δ242-244, R246I in the NTD, and K417N in the RBD) exhibit decreased binding. Of note, the K417N mutation that reduced ACE2 binding (Fig 1C), also significantly impacted plasma recognition by ~1.75-fold compared to D614G (Fig 4C).

Polyclonal recognition of the P.1 Spike was reduced by ~1.33 folds (Fig 4D). Our results show that all the NTD mutations, namely L18F, T20N, P26S, D138Y and R190S, attenuated the binding of naïve-vaccinated plasma Abs (Fig 4D). Furthermore, H655Y also contributed to the immuno-evasive phenotype of the full Spike (Fig 4D). Again, N501Y is the only mutation that increased plasma recognition, indicating its major role amongst all the mutations of this variant.

Although the full B.1.429 Spike did not show a significant evasion of plasma recognition, all of its mutations presented a significant decrease in plasma binding (Fig 4E). Both its NTD mutations, S13I and W152C, were less efficiently recognized by plasma compared to D614G (Fig 4E). The RBD mutation L452R also presented a minor ~1.16-fold decrease in recognition by plasma from vaccinated individuals. Lastly, the B.1.526 full Spike variant did not significantly affect vaccine-elicited plasma recognition. The same phenotype is applicable to most of its

297 mutations, with the exception of D253G substitution in the NTD, which showed a modest ~1.2-
298 fold decrease in binding (Fig 4F).

299 We then evaluated the recognition of our panel of Spikes (VOC, VOI and single mutants)
300 by plasma from previously-infected vaccinated individuals (plasma recovered three weeks post
301 vaccination), as recently described (Tauzin et al., 2021). When comparing all Spikes from
302 emerging variants, the convalescent plasma pre- and post-first dose vaccination both effectively
303 recognized all tested Spikes (Fig 5A, S1 and S2). Vaccinated convalescent individuals developed
304 Abs that were able to robustly recognize and bind to the emerging variants B.1.1.7, B.1.351,
305 B.1.429 and B.1.526 at a similar level than D614G. Binding was decreased by ~ 1.14 folds for P.1,
306 ~1.3 folds for B.1.617 and by ~ 1.8 and ~1.64 folds for B.1.617.1 and B.1.617.2 Spikes,
307 respectively (Fig 5A).

308 Examining each variant and their single mutations more closely, though full B.1.1.7 Spike
309 did not significantly reduce plasma binding in convalescent post-vaccinated individuals, three of
310 its single mutations, ΔY144, P681H, and S982A significantly affected plasma recognition.
311 Substitution S982A in the S2 showed the most important reduction, by ~2 folds compared to
312 D614G (Fig 5B). Inversely, the deletion ΔH69-V70 and the substitution D1118H slightly enhanced
313 the recognition of this Spike by plasma from previously-infected vaccinated individuals. However,
314 combined together, the B.1.1.7 was recognized similarly to its D614G counterpart by these
315 plasmas.

316 The B.1.351 Spike was efficiently recognized by plasma from previously-infected
317 vaccinated individuals with a single mutation presenting lower detection (A701V) (Fig 5C). In the
318 P.1 Spike we observed mutations in the NTD that decreased recognition (P26S, D138Y, and
319 R190S) (Fig 5D). The Spikes from B.1.429 and B.1.526 were also efficiently recognized. Only the

A701V substitution present in the B.1.526 reduced plasma binding (Fig.5F). Among all tested emerging variants, the Spikes from B.1.617.1 and B.1.617.2 presented the most important decrease in recognition by ~1.8 and ~1.64 folds compared to D614G (Figure 5A)

Altogether, our results highlight the difficulty in predicting the phenotype of a particular variant based on the phenotype of its individual mutations.

Neutralization of Spike variants by plasma from vaccinated individuals

We then determined the neutralization profile of the different emerging variants Spikes using a pseudoviral neutralization assay (Anand et al., 2021; Beaudoin-Bussières et al., 2020; Ding et al., 2020; Gasser et al., 2021; Prévost et al., 2020). For this assay we used plasma from five individuals previously infected with SARS-CoV-2 (on average 8 months post-symptom onset) after one dose of the Pfizer/BioNtech BNT162b2 vaccine (samples were collected 22 days after immunization) (Tauzin et al., 2021). As we described previously (Tauzin et al., 2021), we incubated serial dilutions of plasma with pseudoviruses bearing the different Spikes before adding to HEK 293T target cells stably expressing the human ACE2 receptor (Tauzin et al., 2021). We obtained robust neutralization for all pseudoviral particles, with a modest, but significant decrease in neutralization against pseudoviruses bearing the Spike from B.1.351, B.1.526 and B.1.617.2 lineages, indicating that plasma from previously-infected individuals following a single dose have a relatively good neutralizing activity against emerging variants (Fig 6).

DISCUSSION

In our study, we offer a comparative view examining the ACE2 binding properties of selected circulating variants, and the impact of their single mutations on plasma binding. We observed that Spikes from B.1.1.7, B.1.351, P.1, B.1.429, B.1.526, B.1.617, and B.1.617.2 lineages present increased ACE2 interaction. Consistent with previous reports (Leung et al., 2021; Starr et al., 2020; Washington et al., 2021), the N501Y mutation shared by B.1.1.7, B.1.351, and P.1 variants presented a significant increase for ACE2-Fc binding. While N501Y plays a major role in enhanced transmissibility and infectivity (Liu et al., 2021), variants which do not share this mutation have also gained the increased ACE2 binding by harboring other mutations, such as in the B.1.429 lineage, where the L452R showed higher ACE2 binding.

We also analyzed the impact of temperature in modulating the capacity of Spikes from emerging variants to interact with the viral receptor ACE2. For almost all tested Spikes, we observed a significant increase in ACE2 binding at cold temperature (4 ºC). As recently reported, this could be explained by favorable thermodynamics changes allowing the stabilization of the RBD-ACE2 interface and by modulating the Spike trimer conformation (Prévost et al., 2021). While the D614G Spike necessitates lower temperature for optimal ACE2 interaction, Spikes from the different VOCs and VOIs seem to bypass this requirement to efficiently interact with ACE2 at higher temperature (37 ºC). However, whether improved ACE2 binding at higher temperature facilitates emerging variants transmission and propagation remain to be demonstrated. Interestingly, variants harboring the N501Y mutation displayed improve ACE2 interaction compared to the D614G Spike, independently of the temperature, highlighting the critical impact of this substitution in improving Spike – ACE2 interaction. This reveals the importance of closely monitoring the appearance of this mutation among the current and future emerging variants. The appearance of this substitution could potentially impact the transmission and propagation of recent

363 rapidly spreading emerging variants (such as the B.1.617.2 lineage) that do not harbor this
364 mutation, by enhancing the affinity of their Spike for the ACE2 receptor at cold and warm
365 temperatures.

366 We also found that plasma from vaccinated SARS-CoV-2 naïve and prior-infected
367 individuals efficiently recognized the Spikes from emerging variants. However, as previously
368 shown, plasma from vaccinated previously-infected individuals presented a higher and more
369 robust recognition of all tested Spikes (Fig. S2)(Lucas et al., 2021; Tauzin et al., 2021).
370 Accordingly, plasma from these individuals were able to neutralize pseudoviral particles bearing
371 the different emerging variants Spikes, further highlighting the resilience of the deployed vaccines,
372 which were based on the original Wuhan strain.

373

374 **CONCLUSIONS**

375 Altogether, our results highlight the difficulty in predicting the phenotype of an emerging
376 variant's Spike, either related to ACE2 interaction, antigenic profile, infectivity and transmission
377 based on the sum of the phenotype of single mutants making that particular Spike. Antigenic drift
378 has been and remains a concern of the current pandemic (Callaway, 2021; Prévost and Finzi, 2021)
379 and therefore, closely monitoring the functional properties of emerging variants remains of the
380 utmost importance for vaccine design and to inform public health authorities to better manage the
381 epidemic by implementing preventive interventions to control the spread of highly transmissible
382 virus, and tailoring vaccination campaign .

383

CRediT authorship contribution statement

Shang Yu Gong: Conceptualization, Methodology, Validation, Formal analysis, Investigation, Resources, Writing – original draft, Visualization. **Debashree Chatterjee:** Conceptualization, Methodology, Validation, Formal analysis, Investigation, Resources, Writing – original draft, Visualization. **Jonathan Richard:** Conceptualization, Methodology, Validation, Formal analysis, Investigation, Writing – original draft, Supervision. **Jérémie Prévost:** Conceptualization, Methodology, Resources. **Alexandra Tauzin:** Methodology, Resources, Validation, Formal analysis, Investigation. **Romain Gasser**: Methodology, Resources, Validation, Formal analysis, Investigation. **Dani Vézina:** Resources. **Guillaume Goyette:** Resources. **Gabrielle Gendron-Lepage**: Resources. **Michel Roger:** Resources, Writing - Review & Editing. **Marceline Côté:** Methodology, Writing - Review & Editing, Supervision, Funding acquisition. **Andrés Finzi**: Conceptualization, Methodology, Writing – original draft, Writing – original draft, Visualization, Project administration, Supervision, Funding acquisition.

Acknowledgements

The authors thank the CRCHUM BSL 3 and Flow Cytometry Platforms for their technical assistance and Dr Sandrine Moreira (Laboratoire de Santé Publique du Québec) for helpful discussions. We thank Dr. Stefan Pöhlmann and Dr. Markus Hoffmann (Georg-August University) for the plasmids coding for SARS-CoV-2 WT Spike (Wuhan-Hu-1 strain) and Dr Jason McLellan for the plasmid coding for sACE2 expressor. The CV3-25 antibody was produced using the pTT vector kindly provided by the Canada Research Council.

Funding

This work was supported by le Ministère de l'Économie et de l'Innovation (MEI) du Québec, Programme de soutien aux organismes de recherche et d'innovation to A.F., the Fondation du CHUM, a CIHR foundation grant #352417, an Exceptional Fund COVID-19 from the Canada Foundation for Innovation (CFI) #41027, the Sentinelle COVID Quebec network led by the Laboratoire de Santé Publique du Quebec (LSPQ) in collaboration with Fonds de Recherche du Québec-Santé (FRQS) and Genome Canada – Génome Québec, and by the Ministère de la Santé et des Services Sociaux (MSSS) and MEI. Funding was also provided by a CIHR operating grant Pandemic and Health Emergencies Research/Projet #465175 to A.F. and a CIHR stream 1 and 2 for SARS-CoV-2 Variant Research to A.F. and M.C. M.C. and A.F. are recipients of Tier II Canada Research Chair in Molecular Virology and Antiviral Therapeutics (950-232840), and Retroviral Entry no. RCHS0235 950-232424 respectively. J.P. is supported by a CIHR fellowship. R.G. is supported by a MITACS Accélération postdoctoral fellowship. The funders had no role in study design, data collection and analysis, decision to publish, or preparation of the manuscript.

Declaration of competing interest

The authors declare that they have no known competing financial interests or personal relationships that could have appeared to influence the work reported in this paper.

REFERENCES

Amanat, F., Thapa, M., Lei, T., Ahmed, S.M.S., Adelsberg, D.C., Carreño, J.M., Strohmeier, S., Schmitz, A.J., Zafar, S., Zhou, J.Q., Rijnink, W., Alshammary, H., Borcherding, N., Reiche, A.G., Srivastava, K., Sordillo, E.M., van Bakel, H., Personalized Virology, I., Turner, J.S., Bajic, G., Simon, V., Ellebedy, A.H., Krammer, F., 2021. SARS-CoV-2 mRNA vaccination induces functionally diverse antibodies to NTD, RBD, and S2. Cell.

Anand, S.P., Chen, Y., Prévost, J., Gasser, R., Beaudoin-Bussières, G., Abrams, C.F., Pazgier, M., Finzi, A., 2020. Interaction of Human ACE2 to Membrane-Bound SARS-CoV-1 and SARS-CoV-2 S Glycoproteins. Viruses 12.

Anand, S.P., Prévost, J., Nayrac, M., Beaudoin-Bussières, G., Benlarbi, M., Gasser, R., Brassard, N., Laumaea, A., Gong, S.Y., Bourassa, C., Brunet-Ratnasingham, E., Medjahed, H., Gendron-Lepage, G., Goyette, G., Gokool, L., Morrisseau, C., Bégin, P., Martel-Laferrière, V., Tremblay, C., Richard, J., Bazin, R., Duerr, R., Kaufmann, D.E., Finzi, A., 2021. Longitudinal analysis of humoral immunity against SARS-CoV-2 Spike in convalescent individuals up to 8 months post-symptom onset. Cell Rep Med 2, 100290.

Baden, L.R., El Sahly, H.M., Essink, B., Kotloff, K., Frey, S., Novak, R., Diemert, D., Spector, S.A., Rouphael, N., Creech, C.B., McGettigan, J., Khetan, S., Segall, N., Solis, J., Brosz, A., Fierro, C., Schwartz, H., Neuzil, K., Corey, L., Gilbert, P., Janes, H., Follmann, D., Marovich, M., Mascola, J., Polakowski, L., Ledgerwood, J., Graham, B.S., Bennett, H., Pajon, R., Knightly, C., Leav, B., Deng, W., Zhou, H., Han, S., Ivarsson, M., Miller, J., Zaks, T., 2020. Efficacy and Safety of the mRNA-1273 SARS-CoV-2 Vaccine. New England Journal of Medicine 384, 403-416.

Beaudoin-Bussières, G., Laumaea, A., Anand Sai, P., Prévost, J., Gasser, R., Goyette, G., Medjahed, H., Perreault, J., Tremblay, T., Lewin, A., Gokool, L., Morrisseau, C., Bégin, P., Tremblay, C., Martel-Laferrière, V., Kaufmann Daniel, E., Richard, J., Bazin, R., Finzi, A., Ho David, D., Goff Stephen, P., 2020. Decline of Humoral Responses against SARS-CoV-2 Spike in Convalescent Individuals. mBio 11, e02590-02520.

Callaway, E., 2021. Fast-spreading COVID variant can elude immune responses. Nature 589, 500-501.

CDC, SARS-CoV-2 Variant Classifications and Definitions.

Deng, X., Garcia-Knight, M.A., Khalid, M.M., Servellita, V., Wang, C., Morris, M.K., Sotomayor-González, A., Glasner, D.R., Reyes, K.R., Gliwa, A.S., Reddy, N.P., Sanchez San Martin, C., Federman, S., Cheng, J., Balcerek, J., Taylor, J., Streithorst, J.A., Miller, S., Sreekumar, B., Chen, P.Y., Schulze-Gahmen, U., Taha, T.Y., Hayashi, J.M., Simoneau, C.R., Kumar, G.R., McMahon, S., Lidsky, P.V., Xiao, Y., Hemarajata, P., Green, N.M., Espinosa, A., Kath, C., Haw, M., Bell, J., Hacker, J.K., Hanson, C., Wadford, D.A., Anaya, C., Ferguson, D., Frankino, P.A., Shivram, H., Lareau, L.F., Wyman, S.K., Ott, M., Andino, R., Chiu, C.Y., 2021. Transmission, infectivity, and neutralization of a spike L452R SARS-CoV-2 variant. Cell.

Ding, S., Laumaea, A., Benlarbi, M., Beaudoin-Bussières, G., Gasser, R., Medjahed, H., Pancera, M., Stamatatos, L., McGuire, A.T., Bazin, R., Finzi, A., 2020. Antibody Binding to SARS-CoV-2 S Glycoprotein Correlates with but Does Not Predict Neutralization. Viruses 12.

Dong, E., Du, H., Gardner, L., 2020. An interactive web-based dashboard to track COVID-19 in real time. The Lancet Infectious Diseases 20, 533-534.

ECDC, 2020. Rapid increase of a SARS-CoV-2 variant with multiple spike protein mutations observed in the United Kingdom, Threat Assessment Brief.

ECDC, 2021. Emergence of SARS-CoV-2 B.1.617 variants in India and situation in the EU/EEA, Threat Assessment Brief.

Ferreira, I., Datir, R., Kemp, S., Papa, G., Rakshit, P., Singh, S., Meng, B., Pandey, R., Ponnusamy, K., Radhakrishnan, V.S., Sato, K., James, L., Agrawal, A., Gupta, R.K., 2021. SARS-CoV-2 B.1.617 emergence and sensitivity to vaccine-elicited antibodies. bioRxiv, 2021.2005.2008.443253.

Gasser, R., Cloutier, M., Prévost, J., Fink, C., Ducas, É., Ding, S., Dussault, N., Landry, P., Tremblay, T., Laforce-Lavoie, A., Lewin, A., Beaudoin-Bussières, G., Laumaea, A., Medjahed, H., Larochelle, C., Richard, J., Dekaban, G.A., Dikeakos, J.D., Bazin, R., Finzi, A., 2021. Major role of IgM in the neutralizing activity of convalescent plasma against SARS-CoV-2. Cell Rep 34, 108790.

Hoffmann, M., Kleine-Weber, H., Schroeder, S., Krüger, N., Herrler, T., Erichsen, S., Schiergens, T.S., Herrler, G., Wu, N.H., Nitsche, A., Müller, M.A., Drosten, C., Pöhlmann, S., 2020. SARS-CoV-2 Cell Entry Depends on ACE2 and TMPRSS2 and Is Blocked by a Clinically Proven Protease Inhibitor. Cell 181, 271-280.e278.

Jackson, L.A., Anderson, E.J., Rouphael, N.G., Roberts, P.C., Makhene, M., Coler, R.N., McCullough, M.P., Chappell, J.D., Denison, M.R., Stevens, L.J., Pruijssers, A.J., McDermott, A., Flach, B., Doria-Rose, N.A., Corbett, K.S., Morabito, K.M., O'Dell, S., Schmidt, S.D., Swanson, P.A., Padilla, M., Mascola, J.R., Neuzil, K.M., Bennett, H., Sun, W., Peters, E., Makowski, M., Albert, J., Cross, K., Buchanan, W., Pikaart-Tautges, R., Ledgerwood, J.E., Graham, B.S., Beigel, J.H., 2020. An mRNA Vaccine against SARS-CoV-2 — Preliminary Report. New England Journal of Medicine 383, 1920-1931.

Jennewein, M.F., MacCamy, A.J., Akins, N.R., Feng, J., Homad, L.J., Hurlburt, N.K., Seydoux, E., Wan, Y.-H., Stuart, A.B., Edara, V.V., Floyd, K., Vanderheiden, A., Mascola, J.R., Doria-Rose, N., Wang, L., Yang, E.S., Chu, H.Y., Torres, J.L., Ozorowski, G., Ward, A.B., Whaley, R.E., Cohen, K.W., Pancera, M., McElrath, M.J., Englund, J.A., Finzi, A., Suthar, M.S., McGuire, A.T., Stamatatos, L., 2021. Isolation and characterization of cross-neutralizing coronavirus antibodies from COVID-19+ subjects. Cell Reports 36, 109353.

Korber, B., Fischer, W.M., Gnanakaran, S., Yoon, H., Theiler, J., Abfalterer, W., Hengartner, N., Giorgi, E.E., Bhattacharya, T., Foley, B., Hastie, K.M., Parker, M.D., Partridge, D.G., Evans, C.M., Freeman, T.M., de Silva, T.I., McDanal, C., Perez, L.G., Tang, H., Moon-Walker, A., Whelan, S.P., LaBranche, C.C., Saphire, E.O., Montefiori, D.C., 2020. Tracking Changes in SARS-CoV-2 Spike: Evidence that D614G Increases Infectivity of the COVID-19 Virus. Cell 182, 812-827.e819.

500 Krammer, F., 2020. SARS-CoV-2 vaccines in development. Nature 586, 516-527.

501 Leung, K., Shum, M.H., Leung, G.M., Lam, T.T., Wu, J.T., 2021. Early transmissibility assessment of the
502 N501Y mutant strains of SARS-CoV-2 in the United Kingdom, October to November 2020.
503 Eurosurveillance 26, 2002106.

504 Liu, Y., Liu, J., Plante, K.S., Plante, J.A., Xie, X., Zhang, X., Ku, Z., An, Z., Scharton, D., Schindewolf,
505 C., Menachery, V.D., Shi, P.-Y., Weaver, S.C., 2021. The N501Y spike substitution enhances SARS-
506 CoV-2 transmission. bioRxiv : the preprint server for biology, 2021.2003.2008.434499.

507 Lucas, C., Vogels, C.B.F., Yildirim, I., Rothman, J., Lu, P., Monteiro, V., Gelhausen, J.R., Campbell, M.,
508 Silva, J., Tabachikova, A., Munker, M.C., Breban, M.I., Fauver, J.R., Mohanty, S., Huang, J., Yale, S.-C.-
509 G.S.I., Shaw, A.C., Ko, A., Omer, S.B., Grubaugh, N.D., Iwasaki, A., 2021. Impact of circulating SARS-
510 CoV-2 variants on mRNA vaccine-induced immunity in uninfected and previously infected individuals.
511 medRxiv, 2021.2007.2014.21260307.

512 Mothes, W., Li, W., Chen, Y., Prevost, J., Ullah, I., Lu, M., Gong, S.Y., Tauzin, A., Gasser, R., Vezina,
513 D., Anand, S.P., Goyette, G., Chaterjee, D., Ding, S., Tolbert, W.D., Grunst, M.W., Bo, Y., Zhang, S.,
514 Richard, J., Zhou, F., Huang, R.K., Esser, L., Zeher, A., Cote, M., Kumar, P., Sodroski, J., Xia, D., Uchil,
515 P.D., Pazgier, M., Finzi, A., 2021. Structural Basis and Mode of Action for Two Broadly Neutralizing
516 Antibodies Against SARS-CoV-2 Emerging Variants of Concern. bioRxiv, 2021.2008.2002.454546.

517 Mulligan, M.J., Lyke, K.E., Kitchin, N., Absalon, J., Gurtman, A., Lockhart, S., Neuzil, K., Raabe, V.,
518 Bailey, R., Swanson, K.A., Li, P., Koury, K., Kalina, W., Cooper, D., Fontes-Garfias, C., Shi, P.Y.,
519 Türeci, Ö., Tompkins, K.R., Walsh, E.E., Frenck, R., Falsey, A.R., Dormitzer, P.R., Gruber, W.C., Şahin,
520 U., Jansen, K.U., 2020. Phase I/II study of COVID-19 RNA vaccine BNT162b1 in adults. Nature 586,
521 589-593.

522 Mwenda M, S.N., Sinyange N, et al., 2021. Detection of B.1.351 SARS-CoV-2 Variant Strain - Zambia,
523 December 2020, Morbidity and Mortality Weekly Report (MMWR). CDC.

524 Plante, J.A., Liu, Y., Liu, J., Xia, H., Johnson, B.A., Lokugamage, K.G., Zhang, X., Muruato, A.E., Zou,
525 J., Fontes-Garfias, C.R., Mirchandani, D., Scharton, D., Bilello, J.P., Ku, Z., An, Z., Kalveram, B.,
526 Freiberg, A.N., Menachery, V.D., Xie, X., Plante, K.S., Weaver, S.C., Shi, P.-Y., 2021. Spike mutation
527 D614G alters SARS-CoV-2 fitness. Nature 592, 116-121.

528 Polack, F.P., Thomas, S.J., Kitchin, N., Absalon, J., Gurtman, A., Lockhart, S., Perez, J.L., Pérez Marc,
529 G., Moreira, E.D., Zerbini, C., Bailey, R., Swanson, K.A., Roychoudhury, S., Koury, K., Li, P., Kalina,
530 W.V., Cooper, D., Frenck, R.W., Hammitt, L.L., Türeci, Ö., Nell, H., Schaefer, A., Ünal, S., Tresnan,
531 D.B., Mather, S., Dormitzer, P.R., Şahin, U., Jansen, K.U., Gruber, W.C., 2020. Safety and Efficacy of
532 the BNT162b2 mRNA Covid-19 Vaccine. New England Journal of Medicine 383, 2603-2615.

533 Prévost, J., Finzi, A., 2021. The great escape? SARS-CoV-2 variants evading neutralizing responses. Cell
534 Host Microbe 29, 322-324.

535 Prévost, J., Gasser, R., Beaudoin-Bussières, G., Richard, J., Duerr, R., Laumaea, A., Anand, S.P.,
536 Goyette, G., Benlarbi, M., Ding, S., Medjahed, H., Lewin, A., Perreault, J., Tremblay, T., Gendron-
537 Lepage, G., Gauthier, N., Carrier, M., Marcoux, D., Piché, A., Lavoie, M., Benoit, A., Loungnarath, V.,
538 Brochu, G., Haddad, E., Stacey, H.D., Miller, M.S., Desforges, M., Talbot, P.J., Maule, G.T.G., Côté, M.,
539 Therrien, C., Serhir, B., Bazin, R., Roger, M., Finzi, A., 2020. Cross-Sectional Evaluation of Humoral
540 Responses against SARS-CoV-2 Spike. Cell Rep Med 1, 100126.

541 Prévost, J., Richard, J., Gasser, R., Ding, S., Fage, C., Anand, S.P., Adam, D., Vergara, N.G., Tauzin, A.,
542 Benlarbi, M., Gong, S.Y., Goyette, G., Privé, A., Moreira, S., Charest, H., Roger, M., Mothes, W.,
543 Pazgier, M., Brochiero, E., Boivin, G., Abrams, C.F., Schön, A., Finzi, A., 2021. Impact of temperature
544 on the affinity of SARS-CoV-2 Spike for ACE2. bioRxiv, 2021.2007.2009.451812.

545 Rambaut, A., Holmes, E.C., O'Toole, Á., Hill, V., McCrone, J.T., Ruis, C., du Plessis, L., Pybus, O.G.,
546 2020. A dynamic nomenclature proposal for SARS-CoV-2 lineages to assist genomic epidemiology.
547 Nature Microbiology 5, 1403-1407.

548 Sadoff, J., Gray, G., Vandebosch, A., Cárdenas, V., Shukarev, G., Grinsztejn, B., Goepfert, P.A., Truyers,
549 C., Fennema, H., Spiessens, B., Offergeld, K., Scheper, G., Taylor, K.L., Robb, M.L., Treanor, J.,
550 Barouch, D.H., Stoddard, J., Ryser, M.F., Marovich, M.A., Neuzil, K.M., Corey, L., Cauwenberghs, N.,
551 Tanner, T., Hardt, K., Ruiz-Guiñazú, J., Le Gars, M., Schuitemaker, H., Van Hoof, J., Struyf, F.,
552 Douoguih, M., 2021a. Safety and Efficacy of Single-Dose Ad26.COV2.S Vaccine against Covid-19. New
553 England Journal of Medicine 384, 2187-2201.

554 Sadoff, J., Le Gars, M., Shukarev, G., Heerwegh, D., Truyers, C., de Groot, A.M., Stoop, J., Tete, S., Van
555 Damme, W., Leroux-Roels, I., Berghmans, P.-J., Kimmel, M., Van Damme, P., de Hoon, J., Smith, W.,
556 Stephenson, K.E., De Rosa, S.C., Cohen, K.W., McElrath, M.J., Cormier, E., Scheper, G., Barouch, D.H.,
557 Hendriks, J., Struyf, F., Douoguih, M., Van Hoof, J., Schuitemaker, H., 2021b. Interim Results of a Phase
558 1–2a Trial of Ad26.COV2.S Covid-19 Vaccine. New England Journal of Medicine.

559 Shang, J., Ye, G., Shi, K., Wan, Y., Luo, C., Aihara, H., Geng, Q., Auerbach, A., Li, F., 2020. Structural
560 basis of receptor recognition by SARS-CoV-2. Nature 581, 221-224.

561 Starr, T.N., Greaney, A.J., Hilton, S.K., Ellis, D., Crawford, K.H.D., Dingens, A.S., Navarro, M.J.,
562 Bowen, J.E., Tortorici, M.A., Walls, A.C., King, N.P., Veesler, D., Bloom, J.D., 2020. Deep Mutational
563 Scanning of SARS-CoV-2 Receptor Binding Domain Reveals Constraints on Folding and ACE2 Binding.
564 Cell 182, 1295-1310.e1220.

565 Tauzin, A., Nayrac, M., Benlarbi, M., Gong, S.Y., Gasser, R., Beaudoin-Bussières, G., Brassard, N.,
566 Laumaea, A., Vézina, D., Prévost, J., Anand, S.P., Bourassa, C., Gendron-Lepage, G., Medjahed, H.,
567 Goyette, G., Niessl, J., Tastet, O., Gokool, L., Morrisseau, C., Arlotto, P., Stamatatos, L., McGuire, A.T.,
568 Larochelle, C., Uchil, P., Lu, M., Mothes, W., De Serres, G., Moreira, S., Roger, M., Richard, J., Martel-
569 Laferrière, V., Duerr, R., Tremblay, C., Kaufmann, D.E., Finzi, A., 2021. A single dose of the SARS-
570 CoV-2 vaccine BNT162b2 elicits Fc-mediated antibody effector functions and T cell responses. Cell Host
571 Microbe 29, 1137-1150.e1136.

572 Ullah, I., Prévost, J., Ladinsky, M.S., Stone, H., Lu, M., Anand, S.P., Beaudoin-Bussières, G., Benlarbi,
573 M., Ding, S., Gasser, R., Fink, C., Chen, Y., Tauzin, A., Goyette, G., Bourassa, C., Medjahed, H., Mack,

574 M., Chung, K., Wilen, C.B., Dekaban, G.A., Dikeakos, J.D., Bruce, E.A., Kaufmann, D.E., Stamatatos,
575 L., McGuire, A.T., Richard, J., Pazgier, M., Bjorkman, P.J., Mothes, W., Finzi, A., Kumar, P., Uchil,
576 P.D., 2021. Live imaging of SARS-CoV-2 infection in mice reveals neutralizing antibodies require Fc
577 function for optimal efficacy. bioRxiv.

578 Voysey, M., Clemens, S.A.C., Madhi, S.A., Weckx, L.Y., Folegatti, P.M., Aley, P.K., Angus, B., Baillie,
579 V.L., Barnabas, S.L., Bhorat, Q.E., Bibi, S., Briner, C., Cicconi, P., Collins, A.M., Colin-Jones, R.,
580 Cutland, C.L., Darton, T.C., Dheda, K., Duncan, C.J.A., Emary, K.R.W., Ewer, K.J., Fairlie, L., Faust,
581 S.N., Feng, S., Ferreira, D.M., Finn, A., Goodman, A.L., Green, C.M., Green, C.A., Heath, P.T., Hill, C.,
582 Hill, H., Hirsch, I., Hodgson, S.H.C., Izu, A., Jackson, S., Jenkin, D., Joe, C.C.D., Kerridge, S., Koen, A.,
583 Kwatra, G., Lazarus, R., Lawrie, A.M., Lelliott, A., Libri, V., Lillie, P.J., Mallory, R., Mendes, A.V.A.,
584 Milan, E.P., Minassian, A.M., McGregor, A., Morrison, H., Mujadidi, Y.F., Nana, A., O'Reilly, P.J.,
585 Padayachee, S.D., Pittella, A., Plested, E., Pollock, K.M., Ramasamy, M.N., Rhead, S., Schwarzbold,
586 A.V., Singh, N., Smith, A., Song, R., Snape, M.D., Sprinz, E., Sutherland, R.K., Tarrant, R., Thomson,
587 E.C., Török, M.E., Toshner, M., Turner, D.P.J., Vekemans, J., Villafana, T.L., Watson, M.E.E., Williams,
588 C.J., Douglas, A.D., Hill, A.V.S., Lambe, T., Gilbert, S.C., Pollard, A.J., Aban, M., Abayomi, F.,
589 Abeyskera, K., Aboagye, J., Adam, M., Adams, K., Adamson, J., Adelaja, Y.A., Adewetan, G., Adlou, S.,
590 Ahmed, K., Akhalwaya, Y., Akhalwaya, S., Alcock, A., Ali, A., Allen, E.R., Allen, L., Almeida,
591 T.C.D.S.C., Alves, M.P.S., Amorim, F., Andritsou, F., Anslow, R., Appleby, M., Arbe-Barnes, E.H.,
592 Ariaans, M.P., Arns, B., Arruda, L., Azi, P., Azi, L., Babbage, G., Bailey, C., Baker, K.F., Baker, M.,
593 Baker, N., Baker, P., Baldwin, L., Baleanu, I., Bandeira, D., Bara, A., Barbosa, M.A.S., Barker, D.,
594 Barlow, G.D., Barnes, E., Barr, A.S., Barrett, J.R., Barrett, J., Bates, L., Batten, A., Beadon, K., Beales,
595 E., Beckley, R., Belij-Rammerstorfer, S., Bell, J., Bellamy, D., Bellei, N., Belton, S., Berg, A., Bermejo,
596 L., Berrie, E., Berry, L., Berzenyi, D., Beveridge, A., Bewley, K.R., Bexhell, H., Bhikha, S., Bhorat,
597 A.E., Bhorat, Z.E., Bijker, E., Birch, G., Birch, S., Bird, A., Bird, O., Bisnauthsing, K., Bittaye, M.,
598 Blackstone, K., Blackwell, L., Bletchly, H., Blundell, C.L., Blundell, S.R., Bodalia, P., Boettger, B.C.,
599 Bolam, E., Boland, E., Bormans, D., Borthwick, N., Bowring, F., Boyd, A., Bradley, P., Brenner, T.,
600 Brown, P., Brown, C., Brown-O'Sullivan, C., Bruce, S., Brunt, E., Buchan, R., Budd, W., Bulbulia, Y.A.,
601 Bull, M., Burbage, J., Burhan, H., Burn, A., Buttigieg, K.R., Byard, N., Cabera Puig, I., Calderon, G.,
602 Calvert, A., Camara, S., Cao, M., Cappuccini, F., Cardoso, J.R., Carr, M., Carroll, M.W., Carson-Stevens,
603 A., Carvalho, Y.d.M., Carvalho, J.A.M., Casey, H.R., Cashen, P., Castro, T., Castro, L.C., Cathie, K.,
604 Cavey, A., Cerbino-Neto, J., Chadwick, J., Chapman, D., Charlton, S., Chelysheva, I., Chester, O., Chita,
605 S., Cho, J.-S., Cifuentes, L., Clark, E., Clark, M., Clarke, A., Clutterbuck, E.A., Collins, S.L.K., Conlon,
606 C.P., Connarty, S., Coombes, N., Cooper, C., Cooper, R., Cornelissen, L., Corrah, T., Cosgrove, C., Cox,
607 T., Crocker, W.E.M., Crosbie, S., Cullen, L., Cullen, D., Cunha, D.R.M.F., Cunningham, C., Cuthbertson,
608 F.C., Da Guarda, S.N.F., da Silva, L.P., Damratoski, B.E., Danos, Z., Dantas, M.T.D.C., Darroch, P.,
609 Datoo, M.S., Datta, C., Davids, M., Davies, S.L., Davies, H., Davis, E., Davis, J., Davis, J., De Nobrega,
610 M.M.D., De Oliveira Kalid, L.M., Dearlove, D., Demissie, T., Desai, A., Di Marco, S., Di Maso, C.,
611 Dinelli, M.I.S., Dinesh, T., Docksey, C., Dold, C., Dong, T., Donnellan, F.R., Dos Santos, T., dos Santos,
612 T.G., Dos Santos, E.P., Douglas, N., Downing, C., Drake, J., Drake-Brockman, R., Driver, K., Drury, R.,
613 Dunachie, S.J., Durham, B.S., Dutra, L., Easom, N.J.W., van Eck, S., Edwards, M., Edwards, N.J., El
614 Muhanna, O.M., Elias, S.C., Elmore, M., English, M., Esmail, A., Essack, Y.M., Farmer, E., Farooq, M.,
615 Farrar, M., Farrugia, L., Faulkner, B., Fedosyuk, S., Felle, S., Feng, S., Ferreira Da Silva, C., Field, S.,
616 Fisher, R., Flaxman, A., Fletcher, J., Fofie, H., Fok, H., Ford, K.J., Fowler, J., Fraiman, P.H.A., Francis,
617 E., Franco, M.M., Frater, J., Freire, M.S.M., Fry, S.H., Fudge, S., Furze, J., Fuskova, M., Galian-Rubio,
618 P., Galiza, E., Garlant, H., Gavrila, M., Geddes, A., Gibbons, K.A., Gilbride, C., Gill, H., Glynn, S.,
619 Godwin, K., Gokani, K., Goldoni, U.C., Goncalves, M., Gonzalez, I.G.S., Goodwin, J., Goondiwala, A.,
620 Gordon-Quayle, K., Gorini, G., Grab, J., Gracie, L., Greenland, M., Greenwood, N., Greffrath, J.,
621 Groenewald, M.M., Grossi, L., Gupta, G., Hackett, M., Hallis, B., Hamaluba, M., Hamilton, E., Hamlyn,
622 J., Hammersley, D., Hanrath, A.T., Hanumunthadu, B., Harris, S.A., Harris, C., Harris, T., Harrison, T.D.,

623 Harrison, D., Hart, T.C., Hartnell, B., Hassan, S., Haughney, J., Hawkins, S., Hay, J., Head, I., Henry, J.,
624 Hermosin Herrera, M., Hettle, D.B., Hill, J., Hodges, G., Horne, E., Hou, M.M., Houlihan, C., Howe, E.,
625 Howell, N., Humphreys, J., Humphries, H.E., Hurley, K., Huson, C., Hyder-Wright, A., Hyams, C.,
626 Ikram, S., Ishwarbhai, A., Ivan, M., Iveson, P., Iyer, V., Jackson, F., De Jager, J., Jaumdally, S., Jeffers,
627 H., Jesudason, N., Jones, B., Jones, K., Jones, E., Jones, C., Jorge, M.R., Jose, A., Joshi, A., Júnior,
628 E.A.M.S., Kadziola, J., Kailath, R., Kana, F., Karampatsas, K., Kasanyinga, M., Keen, J., Kelly, E.J.,
629 Kelly, D.M., Kelly, D., Kelly, S., Kerr, D., Kfouri, R.d.Á., Khan, L., Khozoee, B., Kidd, S., Killen, A.,
630 Kinch, J., Kinch, P., King, L.D.W., King, T.B., Kingham, L., Klenerman, P., Knapper, F., Knight, J.C.,
631 Knott, D., Koleva, S., Lang, M., Lang, G., Larkworthy, C.W., Larwood, J.P.J., Law, R., Lazarus, E.M.,
632 Leach, A., Lees, E.A., Lemm, N.-M., Lessa, A., Leung, S., Li, Y., Lias, A.M., Liatsikos, K., Linder, A.,
633 Lipworth, S., Liu, S., Liu, X., Lloyd, A., Lloyd, S., Loew, L., Lopez Ramon, R., Lora, L., Lowthorpe, V.,
634 Luz, K., MacDonald, J.C., MacGregor, G., Madhavan, M., Mainwaring, D.O., Makambwa, E., Makinson,
635 R., Malahleha, M., Malamatsho, R., Mallett, G., Mansatta, K., Maoko, T., Mapetla, K., Marchevsky,
636 N.G., Marinou, S., Marlow, E., Marques, G.N., Marriott, P., Marshall, R.P., Marshall, J.L., Martins, F.J.,
637 Masenya, M., Masilela, M., Masters, S.K., Mathew, M., Matlebjane, H., Matshidiso, K., Mazur, O.,
638 Mazzella, A., McCaughan, H., McEwan, J., McGlashan, J., McInroy, L., McIntyre, Z., McLenaghan, D.,
639 McRobert, N., McSwiggan, S., Megson, C., Mehdipour, S., Meijs, W., Mendonça, R.N.Á., Mentzer, A.J.,
640 Mirtorabi, N., Mitton, C., Mnyakeni, S., Moghaddas, F., Molapo, K., Moloi, M., Moore, M., Moraes-
641 Pinto, M.I., Moran, M., Morey, E., Morgans, R., Morris, S., Morris, S., Morris, H.C., Morselli, F.,
642 Morshead, G., Morter, R., Mottal, L., Moultrie, A., Moya, N., Mpelembue, M., Msomi, S., Mugodi, Y.,
643 Mukhopadhyay, E., Muller, J., Munro, A., Munro, C., Murphy, S., Mweu, P., Myasaki, C.H., Naik, G.,
644 Naker, K., Nastouli, E., Nazir, A., Ndlovu, B., Neffa, F., Njenga, C., Noal, H., Noé, A., Novaes, G.,
645 Nugent, F.L., Nunes, G., O'Brien, K., O'Connor, D., Odam, M., Oelofse, S., Oguti, B., Olchawski, V.,
646 Oldfield, N.J., Oliveira, M.G., Oliveira, C., Oosthuizen, A., O'Reilly, P., Osborne, P., Owen, D.R.J.,
647 Owen, L., Owens, D., Owino, N., Pacurar, M., Paiva, B.V.B., Palhares, E.M.F., Palmer, S., Parkinson, S.,
648 Parracho, H.M.R.T., Parsons, K., Patel, D., Patel, B., Patel, F., Patel, K., Patrick-Smith, M., Payne, R.O.,
649 Peng, Y., Penn, E.J., Pennington, A., Peralta Alvarez, M.P., Perring, J., Perry, N., Perumal, R., Petkar, S.,
650 Philip, T., Phillips, D.J., Phillips, J., Phohu, M.K., Pickup, L., Pieterse, S., Piper, J., Pipini, D., Plank, M.,
651 Du Plessis, J., Pollard, S., Pooley, J., Pooran, A., Poulton, I., Powers, C., Presa, F.B., Price, D.A., Price,
652 V., Primeira, M., Proud, P.C., Provstgaard-Morys, S., Pueschel, S., Pulido, D., Quaid, S., Rabara, R.,
653 Radford, A., Radia, K., Rajapaska, D., Rajeswaran, T., Ramos, A.S.F., Ramos Lopez, F., Rampling, T.,
654 Rand, J., Ratcliffe, H., Rawlinson, T., Rea, D., Rees, B., Reiné, J., Resuello-Dauti, M., Reyes Pabon, E.,
655 Ribiero, C.M., Ricamara, M., Richter, A., Ritchie, N., Ritchie, A.J., Robbins, A.J., Roberts, H., Robinson,
656 R.E., Robinson, H., Rocchetti, T.T., Rocha, B.P., Roche, S., Rollier, C., Rose, L., Ross Russell, A.L.,
657 Rossouw, L., Royal, S., Rudiansyah, I., Ruiz, S., Saich, S., Sala, C., Sale, J., Salman, A.M., Salvador, N.,
658 Salvador, S., Sampaio, M., Samson, A.D., Sanchez-Gonzalez, A., Sanders, H., Sanders, K., Santos, E.,
659 Santos Guerra, M.F.S., Satti, I., Saunders, J.E., Saunders, C., Sayed, A., Schim van der Loeff, I., Schmid,
660 A.B., Schofield, E., Screaton, G., Seddiqi, S., Segireddy, R.R., Senger, R., Serrano, S., Shah, R., Shaik, I.,
661 Sharpe, H.E., Sharrocks, K., Shaw, R., Shea, A., Shepherd, A., Shepherd, J.G., Shiham, F., Sidhom, E.,
662 Silk, S.E., da Silva Moraes, A.C., Silva-Junior, G., Silva-Reyes, L., Silveira, A.D., Silveira, M.B.V.,
663 Sinha, J., Skelly, D.T., Smith, D.C., Smith, N., Smith, H.E., Smith, D.J., Smith, C.C., Soares, A., Soares,
664 T., Solórzano, C., Sorio, G.L., Sorley, K., Sosa-Rodriguez, T., Souza, C.M.C.D.L., Souza, B.S.D.F.,
665 Souza, A.R., Spencer, A.J., Spina, F., Spoors, L., Stafford, L., Stamford, I., Starinskij, I., Stein, R.,
666 Steven, J., Stockdale, L., Stockwell, L.V., Strickland, L.H., Stuart, A.C., Sturdy, A., Sutton, N., Szigeti,
667 A., Tahiri-Alaoui, A., Tanner, R., Taoushanis, C., Tarr, A.W., Taylor, K., Taylor, U., Taylor, I.J., Taylor,
668 J., te Water Naude, R., Themistocleous, Y., Themistocleous, A., Thomas, M., Thomas, K., Thomas, T.M.,
669 Thombrayil, A., Thompson, F., Thompson, A., Thompson, K., Thompson, A., Thomson, J., Thornton-
670 Jones, V., Tighe, P.J., Tinoco, L.A., Tiongson, G., Tladinyane, B., Tomasicchio, M., Tomic, A., Tonks,
671 S., Towner, J., Tran, N., Tree, J., Trillana, G., Trinham, C., Trivett, R., Truby, A., Tsheko, B.L., Turabi,
672 A., Turner, R., Turner, C., Ulaszewska, M., Underwood, B.R., Varughese, R., Verbart, D., Verheul, M.,
673 Vichos, I., Vieira, T., Waddington, C.S., Walker, L., Wallis, E., Wand, M., Warbick, D., Wardell, T.,

674 Warimwe, G., Warren, S.C., Watkins, B., Watson, E., Webb, S., Webb-Bridges, A., Webster, A., Welch,
675 J., Wells, J., West, A., White, C., White, R., Williams, P., Williams, R.L., Winslow, R., Woodyer, M.,
676 Worth, A.T., Wright, D., Wroblewska, M., Yao, A., Zimmer, R., Zizi, D., Zuidewind, P., 2021. Safety
677 and efficacy of the ChAdOx1 nCoV-19 vaccine (AZD1222) against SARS-CoV-2: an interim analysis of
678 four randomised controlled trials in Brazil, South Africa, and the UK. The Lancet 397, 99-111.

679 Walls, A.C., Park, Y.J., Tortorici, M.A., Wall, A., McGuire, A.T., Veesler, D., 2020. Structure, Function,
680 and Antigenicity of the SARS-CoV-2 Spike Glycoprotein. Cell 181, 281-292.e286.

681 Walls, A.C., Xiong, X., Park, Y.J., Tortorici, M.A., Snijder, J., Quispe, J., Cameroni, E., Gopal, R., Dai,
682 M., Lanzavecchia, A., Zambon, M., Rey, F.A., Corti, D., Veesler, D., 2019. Unexpected Receptor
683 Functional Mimicry Elucidates Activation of Coronavirus Fusion. Cell 176, 1026-1039.e1015.

684 Wang, P., Nair, M.S., Liu, L., Iketani, S., Luo, Y., Guo, Y., Wang, M., Yu, J., Zhang, B., Kwong, P.D.,
685 Graham, B.S., Mascola, J.R., Chang, J.Y., Yin, M.T., Sobieszczyk, M., Kyratsous, C.A., Shapiro, L.,
686 Sheng, Z., Huang, Y., Ho, D.D., 2021. Antibody resistance of SARS-CoV-2 variants B.1.351 and B.1.1.7.
687 Nature 593, 130-135.

688 Washington, N.L., Gangavarapu, K., Zeller, M., Bolze, A., Cirulli, E.T., Schiabor Barrett, K.M., Larsen,
689 B.B., Anderson, C., White, S., Cassens, T., Jacobs, S., Levan, G., Nguyen, J., Ramirez, J.M., III, Rivera-
690 Garcia, C., Sandoval, E., Wang, X., Wong, D., Spencer, E., Robles-Sikisaka, R., Kurzban, E., Hughes,
691 L.D., Deng, X., Wang, C., Servellita, V., Valentine, H., De Hoff, P., Seaver, P., Sathe, S., Gietzen, K.,
692 Sickler, B., Antico, J., Hoon, K., Liu, J., Harding, A., Bakhtar, O., Basler, T., Austin, B., MacCannell, D.,
693 Isaksson, M., Febbo, P.G., Becker, D., Laurent, M., McDonald, E., Yeo, G.W., Knight, R., Laurent, L.C.,
694 de Feo, E., Worobey, M., Chiu, C.Y., Suchard, M.A., Lu, J.T., Lee, W., Andersen, K.G., 2021.
695 Emergence and rapid transmission of SARS-CoV-2 B.1.1.7 in the United States. Cell 184, 2587-
696 2594.e2587.

697 West, A.P., Wertheim, J.O., Wang, J.C., Vasylyeva, T.I., Havens, J.L., Chowdhury, M.A., Gonzalez, E.,
698 Fang, C.E., Di Lonardo, S.S., Hughes, S., Rakeman, J.L., Lee, H.H., Barnes, C.O., Gnanapragasam,
699 P.N.P., Yang, Z., Gaebler, C., Caskey, M., Nussenzweig, M.C., Keeffe, J.R., Bjorkman, P.J., 2021.
700 Detection and characterization of the SARS-CoV-2 lineage B.1.526 in New York. bioRxiv,
701 2021.2002.2014.431043.

702 Wrapp, D., Wang, N., Corbett, K.S., Goldsmith, J.A., Hsieh, C.L., Abiona, O., Graham, B.S., McLellan,
703 J.S., 2020. Cryo-EM structure of the 2019-nCoV spike in the prefusion conformation. Science 367, 1260-
704 1263.

705 Zhu, X., Mannar, D., Srivastava, S.S., Berezuk, A.M., Demers, J.P., Saville, J.W., Leopold, K., Li, W.,
706 Dimitrov, D.S., Tuttle, K.S., Zhou, S., Chittori, S., Subramaniam, S., 2021. Cryo-electron microscopy
707 structures of the N501Y SARS-CoV-2 spike protein in complex with ACE2 and 2 potent neutralizing
708 antibodies. PLoS Biol 19, e3001237.

709

710

Figure legends

Figure 1. Evaluation hACE2 Fc binding to SARS-CoV-2 Spike variants

HEK 293T cells were transfected to express the indicated SARS-CoV-2 Spike variants. Two days post transfection, cells were stained with ACE2-Fc or with CV3-25 Ab as Spike expression control and analyzed by flow cytometry. ACE2-Fc binding to (A) full Spikes variants or the (B) B.1.1.7, (C) B.1.351, (D) P.1, (E) B.1.429, and (F) B.1.526 Spike and its corresponding single mutations are presented as a ratio of ACE2 binding to D614G Spike normalized to CV3-25 binding. Error bars indicate means ± SEM. Statistical significance has been performed using Mann-Whitney U test according to normality analysis (*$p < 0.05$; **$p < 0.01$; ***$p < 0.001$; ****$p < 0.0001$).

Figure 2. Kinetic Analysis of RBD interaction to hACE2 Binding by Biolayer Interferometry

Association of the different RBD proteins to sACE2 was carried out for 180s at various concentrations in a two-fold dilution series from 500nM to 31.25nM prior to dissociation for 300s for (A) WT, (B) N501Y, (C) K417N, (D) K417T, (F) E484K, and (G)L452R. Curve fitting was performed using a 1:1 binding model in the ForteBio data analysis software. Calculation of on-rates (K_a), off-rates (K_{dis}), and affinity constants (K_D) was computed using a global fit applied to all data. Raw data are presented in blue and fitting models are in red. Results are summarized in Table S1.

Figure 3. Evaluation of the impact of temperature on Spike-ACE2 interaction.

HEK 293T cells were transfected with the indicated SARS-CoV-2 Spike variants. Two days post transfection, cells were stained with ACE2-Fc or with CV3-25 Ab as Spike expression control at

735 4ºC or 37ºC and analyzed by flow cytometry. ACE2-Fc binding to the different Spike variants are
736 presented as a ratio of ACE2 binding to D614G Spik, normalized to CV3-25 binding at 37ºC (red)
737 or at 4ºC (blue). Statistical analyses were used to compare each Spike at 4ºC vs 37ºC (black) or to
738 compare variants Spike to D614G at 37ºC (red) or at 4ºC (blue). Fold changes of ACE2 binding at
739 4ºC vs 37ºC for each Spike is shown in black. Error bars indicate means ± SEM. Statistical
740 significance has been performed using Mann-Whitney U test (*$p < 0.05$; **$p < 0.01$; ***$p < 0.001$;
741 ****$p < 0.0001$, ns; non-significant).
742
743 **Figure 4. Recognition of SARS-CoV-2 Spike variants and single mutants by plasma from**
744 **vaccinated SARS-CoV-2 naïve individuals.**
745 HEK 293T cells were transfected with the indicated SARS-CoV-2 spike variants. Two days post
746 transfection, cells were stained with 1:250 dilution of plasma collected from naive post vaccinated
747 individuals (n=3-5) or with CV3-25 Ab as control and analyzed by flow cytometry. Plasma
748 recognition of (A) full Spike variants (B) B.1.1.7, (C) B.1.351, (D) P.1, (E) B.1.429, (F) B.1.526
749 Spike and variant-specific Spike single mutations are presented as ratio of plasma binding to
750 D614G Spike normalized CV3-25 binding. Error bars indicate means± SEM. Statistical
751 significance has been performed using Mann-Whitney U test (*$p < 0.05$; **$p < 0.01$; ***$p < 0.001$;
752 ****$p < 0.0001$).
753
754 **Figure 5. Recognition of SARS-CoV-2 Spike variants and single mutants by plasma from**
755 **vaccinated previously-infected individuals.**
756 HEK293T cells were transfected with SARS-CoV-2 full Spike variants and stained with plasma
757 collected 3 weeks post-first dose vaccinated previously infected individuals (n=3-5) or with CV3-

25 Ab and analyzed by flow cytometry. Plasma recognition of (A) full Spike variants or the (B) B.1.1.7, (C) B.1.351, (D) P.1, (E) B.1.429, (F) B.1.526 Spikes and Spikes with their corresponding single mutations are presented as a ratio of plasma binding to D614G Spike normalized with CV3-25 binding. Error bars indicate means ± SEM. Statistical significance has been performed using Mann-Whitney U test (*$p < 0.05$; **$p < 0.01$; ***$p < 0.001$; ****$p < 0.0001$).

Figure 6. Neutralization of SARS-CoV-2 Spike variants by plasma from previously infected vaccinated individuals

Neutralizing activity of previously infected vaccinated individuals against pseudoviruses bearing the SARS-CoV-2 Spike variants were assessed. Pseudoviruses with serial dilutions of plasma were incubate for 1 h at 37°C before infecting 293T-ACE2 cells. ID_{50} against pseudoviruses were calculated by a normalized non-linear regression using GraphPad Prism software. Detection limit is indicated in the graph (ID_{50}=50). Statistical significance has been performed using Mann-Whitney U test (*$p < 0.05$).

SUPPLEMENTAL TABLE

Table S1. Binding Kinetics of the interaction between SARS-CoV-2 RBD and sACE2 quantified by Biolayer Interferometry.

Table S2. Summary of ACE2 Binding, Plasma binding, and Neutralization to Spike variants.

SUPPLEMENTAL FIGURES

Figure S1. Recognition of SARS-CoV-2 Spike variants and single mutants by plasma from convalescent donors.

HEK293T cells were transfected with the indicated SARS-CoV-2 spike variants and stained with plasma collected from individuals that were infected around 9 months before plasma collection (n=5) or with CV3-25Ab and analyzed by flow cytometry. Plasma recognition of (A) full Spike variants or the (B) B.1.1.7, (C) B.1.351, (D) P.1, (E) B.1.429, (F) B.1.526 Spikes and lineage specific Spike single mutations are presented as ratio of plasma binding to D614G normalized with CV3-25 binding. Error bars indicate means± SEM. Statistical significance has been performed using Mann-Whitney U test (*$p < 0.05$; **$p < 0.01$; ***$p < 0.001$; ****$p < 0.0001$).

Figure S2. Recognition of SARS-CoV-2 Spike variants by plasma from naïve or previously-infected, vaccinated individuals.

HEK293T cells were transfected with SARS-CoV-2 full Spike variants and stained with plasma collected 3 weeks post-first dose vaccinated previously infected individuals (n=5), first dose vaccinated naïve individuals (n=5), or CV3-25 Ab and analyzed by flow cytometry. Plasma recognition of full Spike variants are represented as Median Fluorescent Intensities (MFIs)

796 normalized as a percentage of CV3-25 binding. Error bars indicate means ± SEM. Statistical
797 significance has been performed using Mann-Whitney U test (*$p < 0.05$; **$p < 0.01$; ***$p < 0.001$;
798 ****$p < 0.0001$).
799

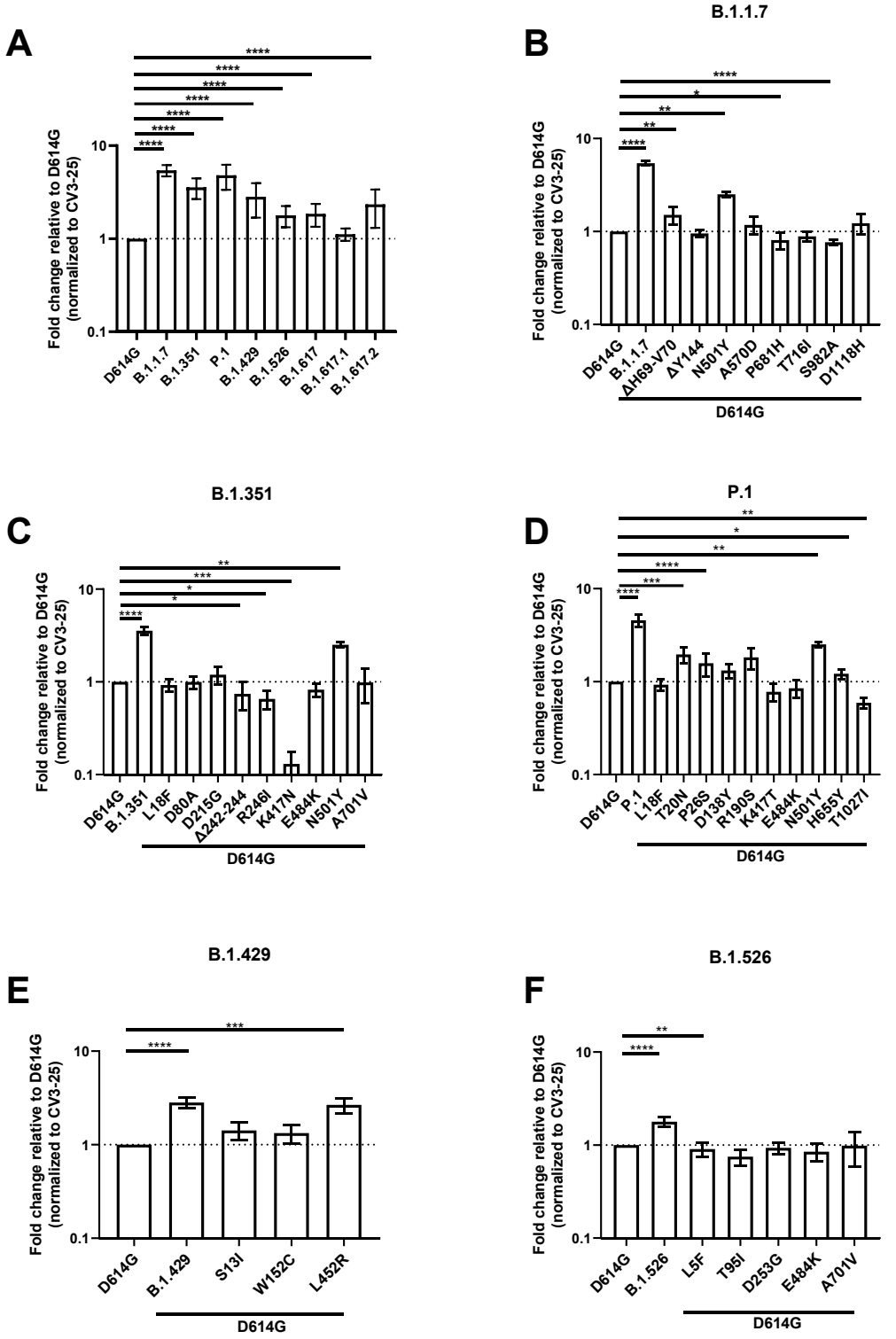
A
Fold change relative to D614G (normalized to CV3-25)
D614G
B.1.1.7
B.1.351
P.1
B.1.429
B.1.526
B.1.617
B.1.617.1
B.1.617.2
B
B.1.1.7
ΔH69-V70
ΔY144
N501Y
A570D
P681H
T716I
S982A
D1118H
D614G
C
B.1.351
L18F
D80A
D215G
Δ242-244
R246I
K417N
E484K
N501Y
A701V
D
P.1
L18F
T20N
P26S
D138Y
R190S
K417T
E484K
N501Y
H655Y
T1027I
E
B.1.429
S13I
W152C
L452R
F
B.1.526
L5F
T95I
D253G
E484K
A701V

Figure 1

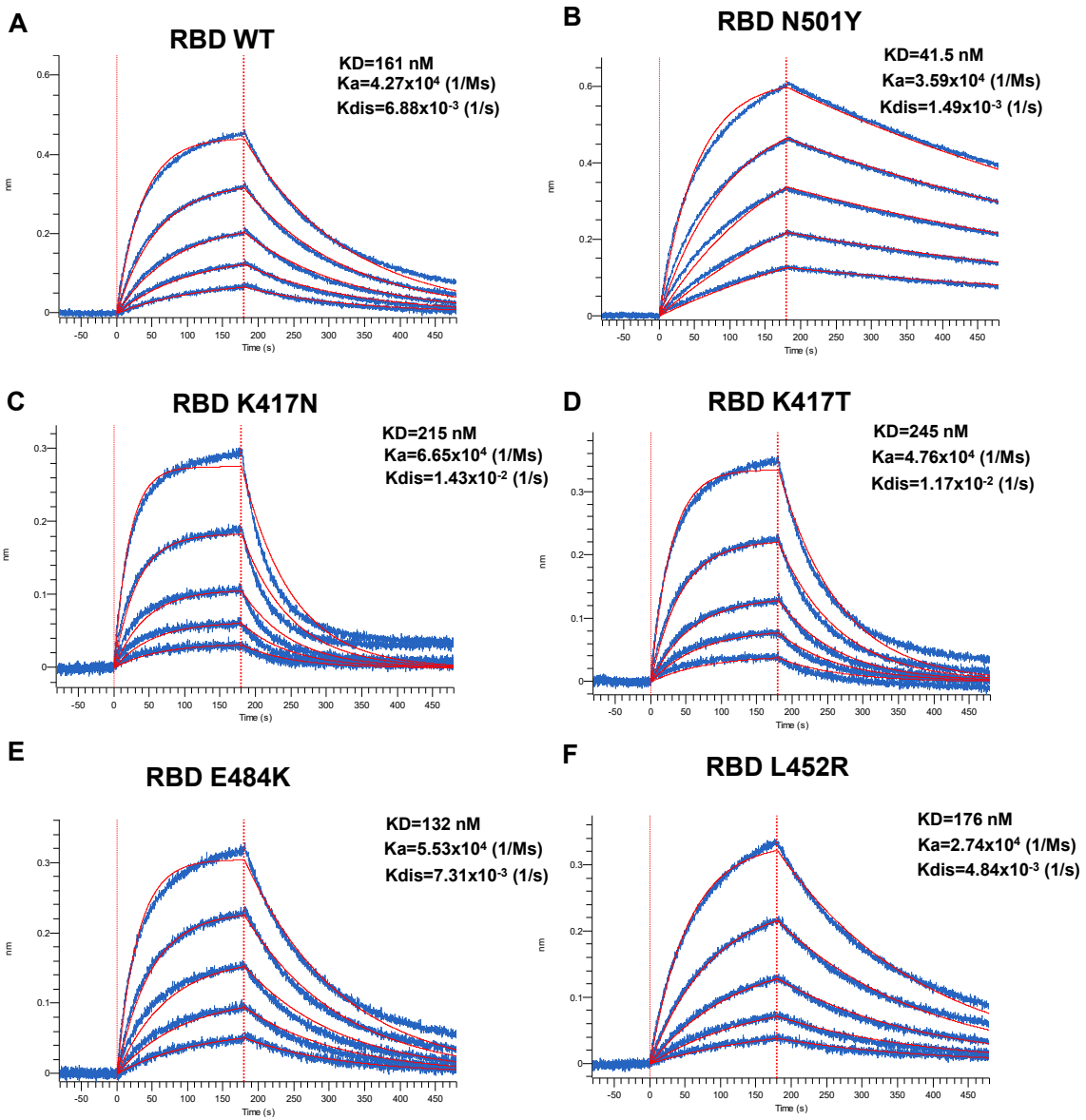
A
RBD WT
KD=161 nM
Ka=4.27x10⁴ (1/Ms)
Kdis=6.88x10⁻³ (1/s)
B
RBD N501Y
KD=41.5 nM
Ka=3.59x10⁴ (1/Ms)
Kdis=1.49x10⁻³ (1/s)
C
RBD K417N
KD=215 nM
Ka=6.65x10⁴ (1/Ms)
Kdis=1.43x10⁻² (1/s)
D
RBD K417T
KD=245 nM
Ka=4.76x10⁴ (1/Ms)
Kdis=1.17x10⁻² (1/s)
E
RBD E484K
KD=132 nM
Ka=5.53x10⁴ (1/Ms)
Kdis=7.31x10⁻³ (1/s)
F
RBD L452R
KD=176 nM
Ka=2.74x10⁴ (1/Ms)
Kdis=4.84x10⁻³ (1/s)
nm
Time (s)

Figure 2

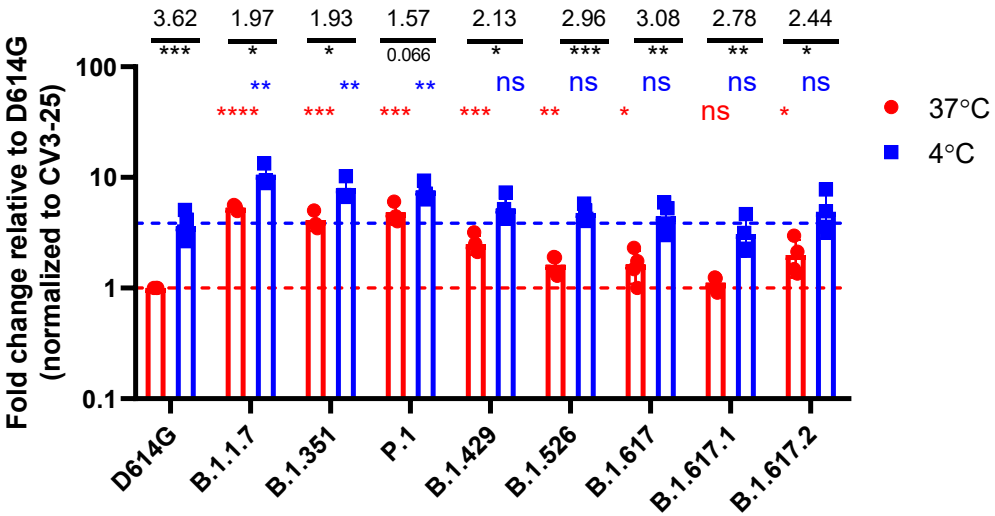
Fold change relative to D614G
(normalized to CV3-25)
100
10
1
0.1
3.62
1.97
1.93
1.57
2.13
2.96
3.08
2.78
2.44
***
*
*
0.066
*
***
**
**
**
ns
ns
ns
ns
ns
****
***
***
***
**
*
ns
*
D614G
B.1.1.7
B.1.351
P.1
B.1.429
B.1.526
B.1.617
B.1.617.1
B.1.617.2
37°C
4°C

Figure 3

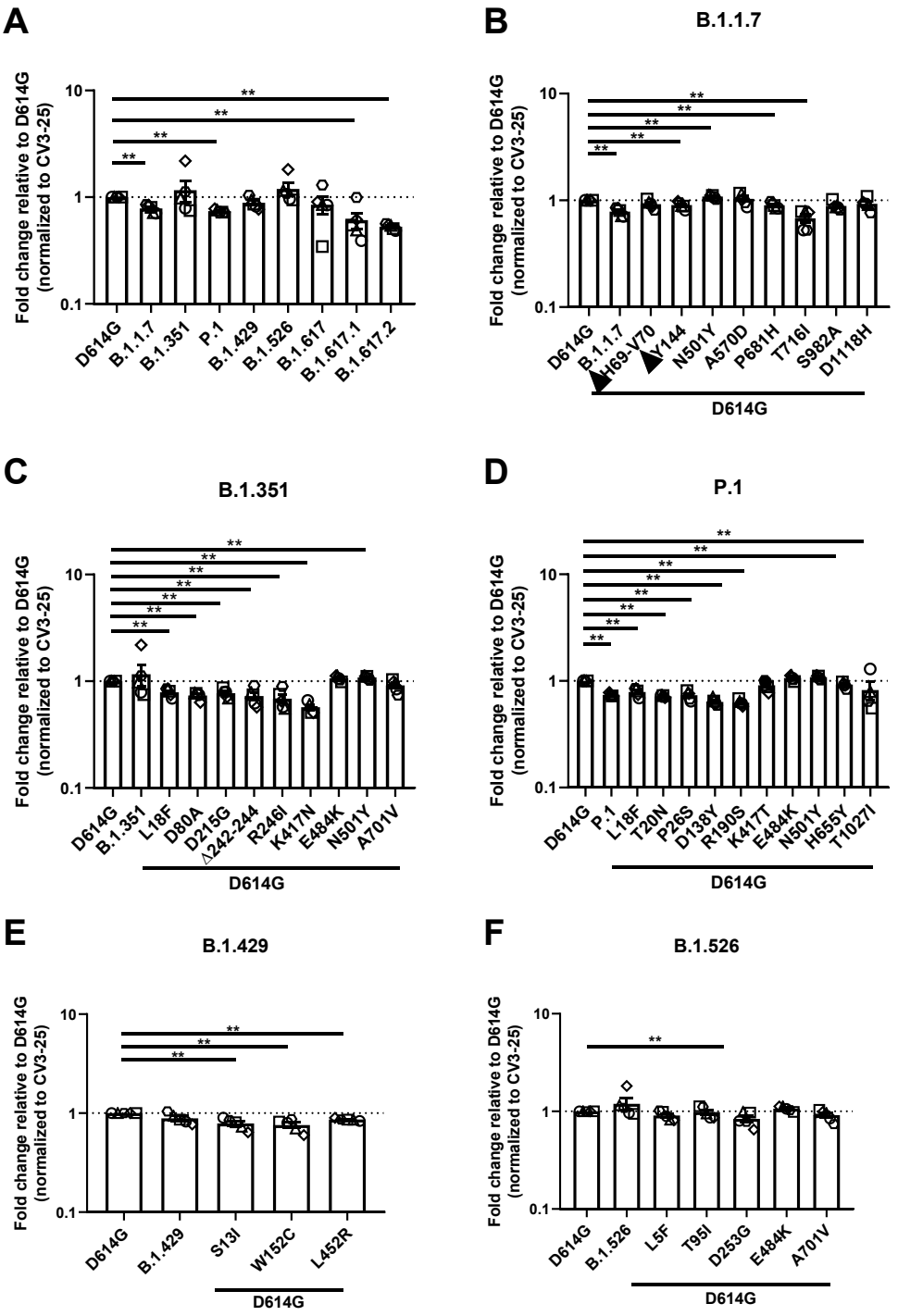
A
Fold change relative to D614G (normalized to CV3-25)
10
1
0.1
**
D614G
B.1.1.7
B.1.351
P.1
B.1.429
B.1.526
B.1.617
B.1.617.1
B.1.617.2
B
B.1.1.7
D614G
B.1.1.7
ΔH69-V70
ΔY144
N501Y
A570D
P681H
T716I
S982A
D1118H
D614G
C
B.1.351
D614G
B.1.351
L18F
D80A
D215G
Δ242-244
R246I
K417N
E484K
N501Y
A701V
D614G
D
P.1
D614G
P.1
L18F
T20N
P26S
D138Y
R190S
K417T
E484K
N501Y
H655Y
T1027I
D614G
E
B.1.429
D614G
B.1.429
S13I
W152C
L452R
D614G
F
B.1.526
D614G
B.1.526
L5F
T95I
D253G
E484K
A701V
D614G

Figure 4

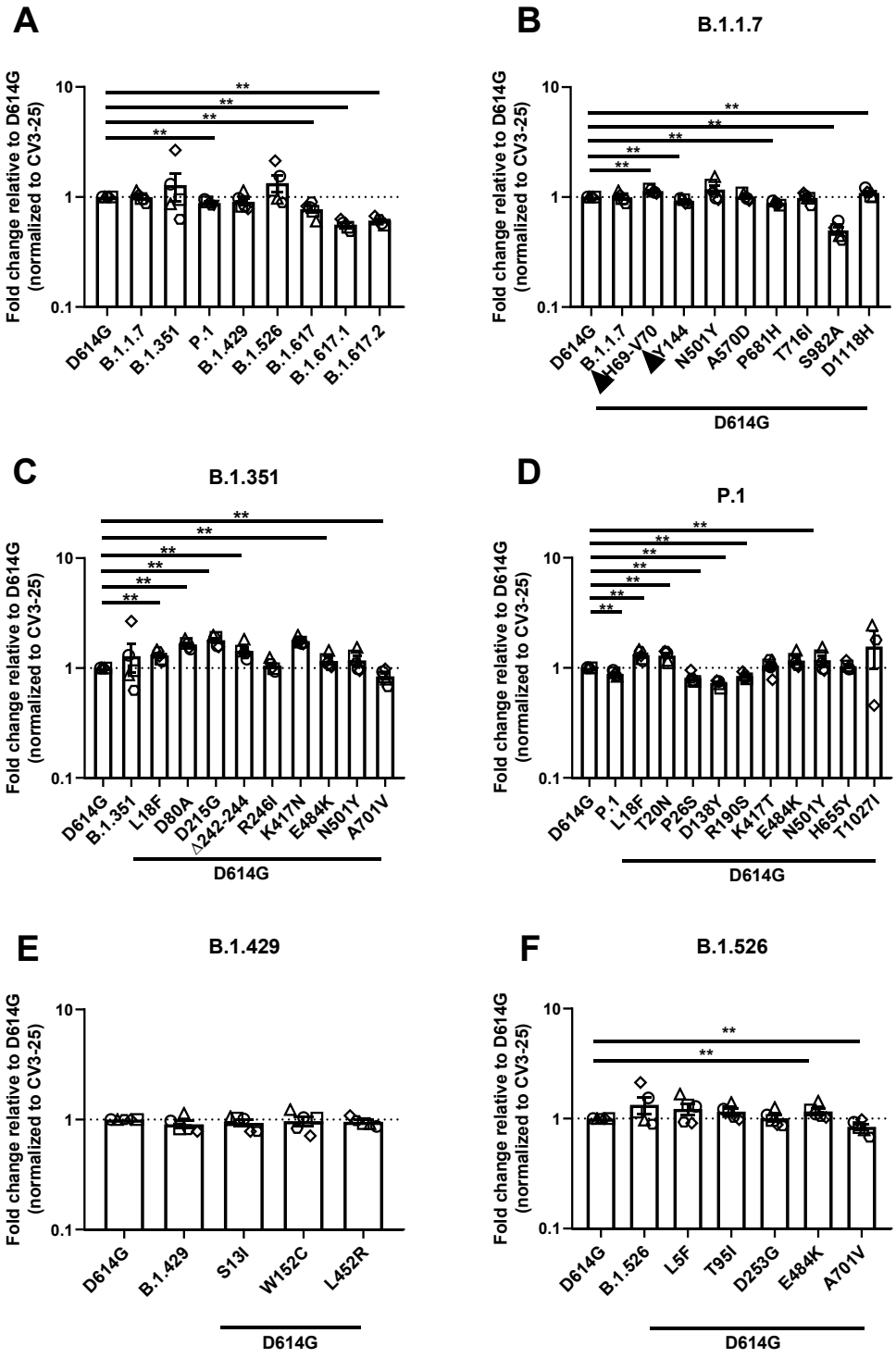
A
Fold change relative to D614G (normalized to CV3-25)
10
1
0.1
**
D614G
B.1.1.7
B.1.351
P.1
B.1.429
B.1.526
B.1.617
B.1.617.1
B.1.617.2
B
B.1.1.7
D614G
B.1.1.7
ΔH69-V70
ΔY144
N501Y
A570D
P681H
T716I
S982A
D1118H
D614G
C
B.1.351
D614G
B.1.351
L18F
D80A
D215G
Δ242-244
R246I
K417N
E484K
N501Y
A701V
D614G
D
P.1
D614G
P.1
L18F
T20N
P26S
D138Y
R190S
K417T
E484K
N501Y
H655Y
T1027I
D614G
E
B.1.429
D614G
B.1.429
S13I
W152C
L452R
D614G
F
B.1.526
D614G
B.1.526
L5F
T95I
D253G
E484K
A701V
D614G

Figure 5

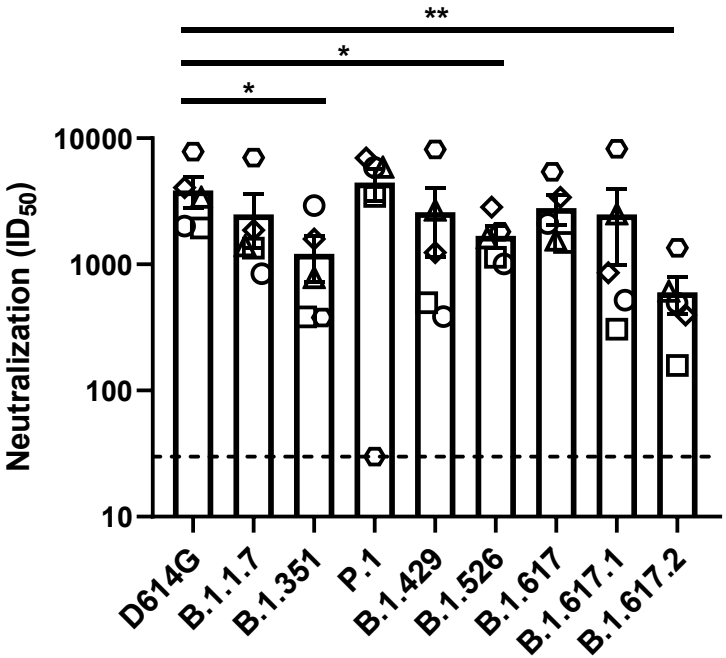
**
*
*
Neutralization (ID50)
10000
1000
100
10
D614G
B.1.1.7
B.1.351
P.1
B.1.429
B.1.526
B.1.617
B.1.617.1
B.1.617.2

Figure 6

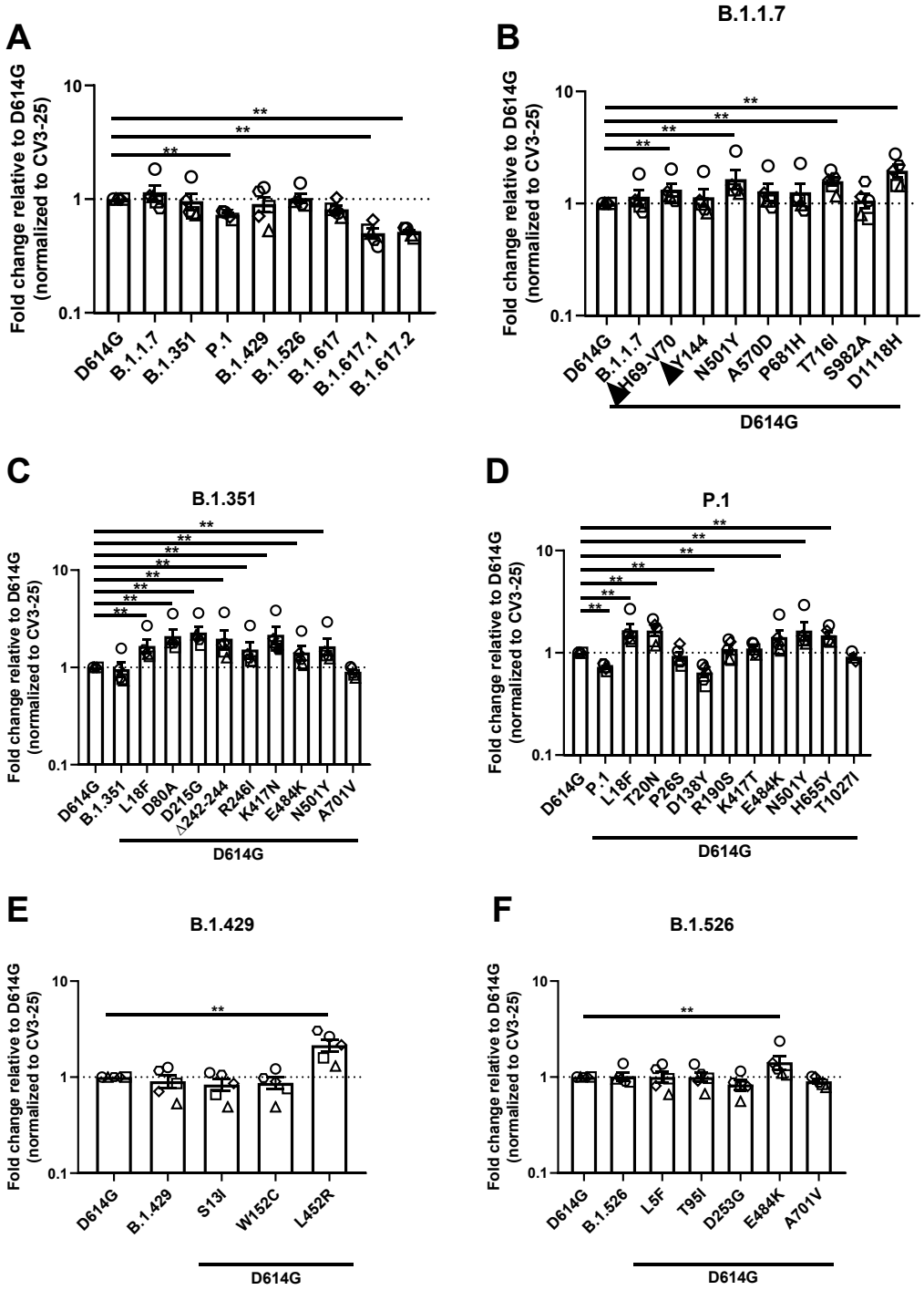
A
Fold change relative to D614G (normalized to CV3-25)
10
1
0.1
**
**
**
D614G
B.1.1.7
B.1.351
P.1
B.1.429
B.1.526
B.1.617
B.1.617.1
B.1.617.2
B
B.1.1.7
Fold change relative to D614G (normalized to CV3-25)
**
**
**
**
D614G
B.1.1.7
H69-V70
Y144
N501Y
A570D
P681H
T716I
S982A
D1118H
D614G
C
B.1.351
Fold change relative to D614G (normalized to CV3-25)
**
**
**
**
**
**
**
**
D614G
B.1.351
L18F
D80A
D215G
Δ242-244
R246I
K417N
E484K
N501Y
A701V
D614G
D
P.1
Fold change relative to D614G (normalized to CV3-25)
**
**
**
**
**
**
**
D614G
P.1
L18F
T20N
P26S
D138Y
R190S
K417T
E484K
N501Y
H655Y
T1027I
D614G
E
B.1.429
Fold change relative to D614G (normalized to CV3-25)
**
D614G
B.1.429
S13I
W152C
L452R
D614G
F
B.1.526
Fold change relative to D614G (normalized to CV3-25)
**
D614G
B.1.526
L5F
T95I
D253G
E484K
A701V
D614G

Figure S1

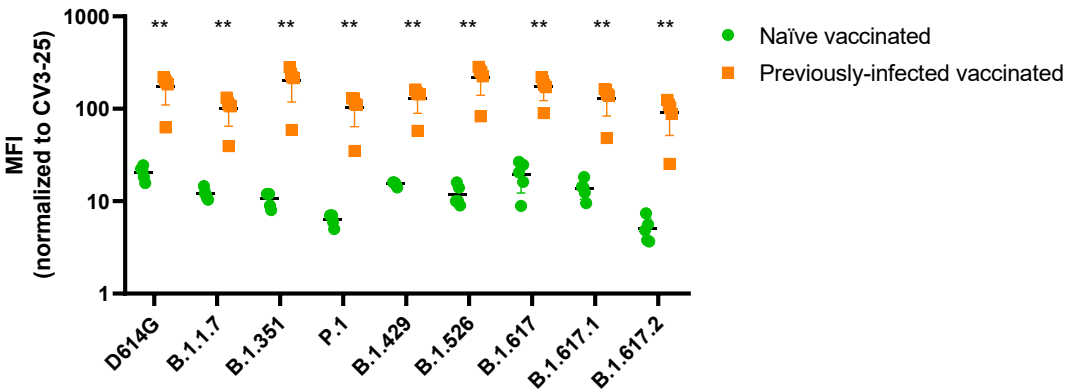
MFI
(normalized to CV3-25)
1000
100
10
1
**
D614G
B.1.1.7
B.1.351
P.1
B.1.429
B.1.526
B.1.617
B.1.617.1
B.1.617.2
Naïve vaccinated
Previously-infected vaccinated

Figure S2

Table S1: Binding Kinetics of the interaction between SARS-CoV-2 RBD and sACE2 quantified by Biolayer Interferometry.

RBD	ACE2 binding (RBD/biolayer interferometry)					
	KD (nM)	Fold change	Ka (1/Ms)	Fold change	Kdis (1/s)	Fold change
WT	161	1	4.27×10^{4}	1	6.88×10^{-3}	1
N501Y	41.5	3.88	3.59×10^{4}	0.84	1.49×10^{-3}	0.22
K417N	215	0.75	6.65×10^{4}	1.56	1.43×10^{-2}	2.07
K417T	245	0.66	4.76×10^{4}	1.11	1.17×10^{-2}	1.70
E484K	132	1.22	5.53×10^{4}	1.29	7.31×10^{-3}	1.06
L452R	176	0.91	2.74×10^{4}	0.64	4.84×10^{-3}	0.70

Table S2. Summary of ACE2 Binding, Plasma binding, and Neutralization to Spike variants.

Variant / mutant		ACE2 binding[a]	Spike recognition by plasma[b]			Neutralization[c] ID50 (ratio to D614G)
			Previously infected (8 months PSO)	Previously infected Vaccinated (3 weeks post-vaccination)	Naïve vaccinated (3 weeks post-vaccination)	
	D614G	1.00	1.00	1.00	1.00	3852 (1)
B.1.1.7	Full variant	5.43	1.15	1.00	0.78	2492 (0.65)
	D614G/Δ69-70	1.51	1.33	1.14	0.92	
	D614G/Δ144	0.95	1.14	0.93	0.90	
	D614G/N501Y	2.52	1.65	1.17	1.09	
	D614G/A570D	1.18	1.29	1.01	1.04	
	D614G/P681H	0.81	1.26	0.88	0.90	
	D614G/T716I	0.89	1.58	0.98	0.68	
	D614G/S982A	0.77	1.06	0.50	0.89	
	D614G/D1118H	1.23	1.96	1.09	0.93	
B.1.351	Full variant	3.56	0.96	1.28	1.17	1211 (0.31)
	D614G/L18F	0.93	1.66	1.30	0.79	
	D614G/D80A	1.00	2.11	1.64	0.74	
	D614G/D215G	1.19	2.29	1.79	0.77	
	D614G/ Δ242-244	0.74	1.97	1.43	0.73	
	D614G/R246I	0.66	1.53	1.05	0.69	
	D614G/K417N	0.13	2.16	1.76	0.57	
	D614G/E484K	0.82	1.42	1.16	1.06	
	D614G/N501Y	2.52	1.65	1.17	1.09	
	D614G/A701V	0.99	0.90	0.84	0.91	
P.1	Full variant	4.24	0.77	0.88	0.79	4445 (1.15)
	D614G/L18F	0.93	1.66	1.30	0.79	
	D614G/T20N	1.96	1.65	1.29	0.72	
	D614G/P26S	1.58	0.93	0.81	0.73	
	D614G/D138Y	1.32	0.64	0.73	0.64	
	D614G/R190S	1.82	1.09	0.84	0.63	
	D614G/K417T	0.78	1.10	1.04	0.91	
	D614G/E484K	0.85	1.42	1.16	1.06	
	D614G/N501Y	2.52	1.65	1.17	1.09	
	D614G/H655Y	1.21	1.48	1.04	0.92	
	D614G/T1027I	0.59	1.56	0.76	0.82	
B.1.526	Full variant	1.78	1.02	1.34	1.19	1686 (0.44)
	D614G/L5F	0.91	1.00	1.23	0.91	
	D614G/T95I	0.75	1.00	1.16	0.98	
	D614G/D253G	0.93	0.84	1.01	0.84	
	D614G/E484K	0.85	1.42	1.16	1.06	
	D614G/A701V	0.99	0.90	0.84	0.91	
B.1.429	Full variant	2.82	0.91	0.90	0.89	2591 (0.67)
	D614G/S13I	1.42	0.84	0.93	0.79	
	D614G/W152C	1.33	0.87	0.97	0.76	
	D614G/L452R	2.66	2.15	0.95	0.86	
B.1.617	Full variant	1.85	0.82	0.77	0.85	2795 (0.73)
B.1.617.1	Full variant	1.12	0.50	0.56	0.61	2489 (0.65)
B.1.617.2	Full variant	2.34	0.52	0.61	0.53	601 (0.16)

a) ACE2-Fc binding was normalized to CV3-25 binding in each experiment. Values are presented as ratio of normalized ACE2-Fc binding obtain with the D614G Spike. Values represent the means of data obtained from at least three independent experiments.

b) Plasma binding were normalized to CV3-25 in each experiment. Values are presented as ratio of normalized plasma binding obtained with the D614G Spike. Values represent the means of data obtained with 3-5 plasma from the same group.

c) The ID50 represents the plasma dilution to inhibit 50% of the infection of 293T-ACE2 cells by recombinant viruses bearing the indicated Spike. Values are presented as the means of ID50 and as ratio of the ID50 obtained with virus bearing the D614G Spike. Values represent the means of data obtained with 3-5 different plasma.